Growth Prediction Based on a Three-Dimensional Assessment of Cervical Vertebrae

by

Greg Charles Miller, D.D.S.

THESIS

Submitted in partial satisfaction of the requirements for the degree of

MASTERS OF SCIENCE

in

ORAL AND CRANIOFACIAL SCIENCES

in the

GRADUATE DIVISION

of the

UNIVERSITY OF CALIFORNIA

San Francisco

[redacted]

Date University Librarian

ACKNOWLEDGEMENTS

None of the work on this project would have been successful without the input and support from various people.

I would like to thank my research committee. Dr. John Huang was instrumental in assisting me to understand the intricacies of the cone beam software. Whenever spending hours sitting in front of a computer caused me to lose sight of the clinical implications of my research Dr. Gerald Nelson was always there to point me in the right direction. I will also be forever indebted to Dr. Art Miller, who spent countless hours helping me to organize my thoughts and to make sense of my data, all the while finding a way to tell me the answers while making me believe I came up with them myself.

Most importantly, I am forever grateful for my wonderful family. Thank you to my wonderful and supportive parents Melvin and Nancy Miller, and my lovely and beautiful wife, Dr. Helaine Kan.

Growth Prediction Based on a Three-Dimensional Assessment of Cervical Vertebrae

Greg Charles Miller, DDS

ABSTRACT

Many studies have investigated skeletal age as a determinant of growth, most notably studying the radiographic morphology of the hand-wrist as well as the cervical vertebrae on lateral headfilms. While a recent investigation evaluated the ability to segment cervical spine units, to date, no study has been published which attempts to assess a patient's growth potential and skeletal age via the use of three-dimensional x-ray technology. This is a key issue as 3-D radiographic assessments are quickly becoming the standard of care in orthodontic treatment.

The purpose of this study was to objectively measure the morphology of cervical vertebrae (C3, C4, and C5) in 14 females and 9 males as imaged on a rendered cone beam computed tomographic image (CBCT). Landmarks were identified and linear and angular measurements were taken. A stepwise regression analysis was performed in order to quantify which measurements changed with age.

The specific aims of this study were to segment 3-D renderings of the cervical vertebrae from a CBCT image, to identify useful landmarks, to correlate vertebral morphology to age, and to assess the reproducibility of a 3-D analysis. The null hypothesis stated that there is no correlation between the 3-D measurements of the cervical vertebrae and age. A linear regression analysis was plotted to compare each measurement to each other, and a formula was developed using a stepwise regression to define which of the measures were most related to the age of the subjects.

The results indicate that there are significant and predicable changes in the morphology of the cervical vertebrae associated with age, and that these changes can be used to predict the skeletal age of a given patient. The strongest correlations between age and morphology were in the anterior (0.77, 0.93, and 0.86, for C3, C4, and C5, respectively) and posterior (0.72, 0.81, and 0.84) vertical body height, and the lower (0.68, 0.82, 0.69) and upper (0.60, 0.80, 0.73) AP angles of all three vertebrae studied. Taking into account the possible variation in size for vertebrae between individuals, an equation was developed. This equation shows that the most predictive factors of age, once size is accounted for, are the C3 upper AP distance, the C4 anterior body vertical height, the C4 upper AP angle, and the C5 upper transverse angle. The value of using three-dimensional measures of the vertebrae is that the foramen size can be used as a indicator of the individual subject's size, and subtracted from the three dimensional measures that relate closest to the age of the subject. Determining the log of the differences allows using numbers of markedly different ranges or sizes. The constants that are used with each measure provide the slope of the relationship of that measure to chronological age. Three-dimensional rendering of the human vertebrae provides a method to accurately determine the age of a subject while accounting for individual differences in size.

TABLE OF CONTENTS

List of Tables

List of Figures

Introduction

Orthodontic treatment in growing children involves treatment during varying stages of growth and development. During this period of patient growth, there is an opportunity to affect changes in the relationships among the skeleton, dentition, and soft tissue. A concept long pursued is to accurately predict the remaining growth potential for a child. The purpose is developing more effective orthopedic change during treatment. Many studies have investigated skeletal age as a determinant of growth, using both hand-wrist and lateral cephalometric radiographs. While a recent investigation evaluated the ability to segment cervical spine units,[1] to date, no study has been published which attempts to assess a patient's growth potential and skeletal age via the use of three-dimensional x-ray technology.

Methods of Assessing Growth

Knowledge of a patient's remaining growth potential facilitates growth modification in order to correct skeletal imbalances. Orthopedic change, which is reliant upon growth modification, will only be successful if attempted prior to the completion of growth. The clinician will ideally initiate treatment just prior to the pubertal growth spurt in order to maximize orthopedic effect by taking advantage of the highest growth velocity.

Age alone is not sufficient for determining the amount of remaining growth. It has been shown that there is little correlation between age and early, average, or late maturation.[2] Numerous studies have evaluated indicators of growth potential and its relationship to age. The following factors have been evaluated: sexual maturation,[3,4] dental maturation,[5,6] height and weight,[7,8] skeletal development,[9,10] and vertebral development.[11-14]

The most commonly used growth maturity indicators are the presence or absence of secondary sexual characteristics and onset of menarche.[15] However, a better indicator for growth potential is an assessment of skeletal age, for which the gold standard is the hand-wrist radiograph.[9] The disadvantage is the extra cost and an extra exposure of radiation for the patient.

Over the past several years, research has indicated that the stage of development of the cervical spine is a useful indicator of skeletal age.[11,12] There are definite sequential growth and maturational changes of the cervical vertebrae which are readily viewable on a lateral cephalogram.[11,12,14,16] One great convenience to clinician and patient in using an analysis of the cervical vertebrae to assess growth is that the lateral head film is a standard radiograph taken prior to the start of orthodontic treatment. Additional cost and radiation exposure is unnecessary. Furthermore, several studies have shown that the cervical vertebral changes are as predictable as those seen on a hand-wrist, thereby confirming that a vertebral analysis is as reliable as a hand-wrist analysis.[14,17-20]

Anatomy of the Vertebrae

The cervical spine is comprised of seven vertebrae, numbered from the most superior to the most inferior, C1-C7. C1 and C2 are each unique, whereas C3-C7 are similar in appearance. Figures 1 and 2 demonstrate the anatomy of the human cervical vertebrae from C3-C7.

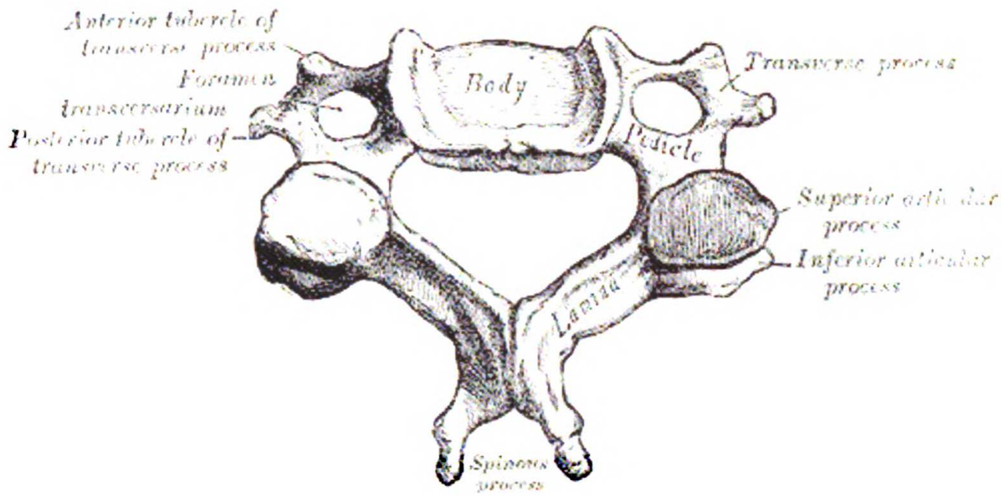

Figure 1: A schematic of an adult human cervical vertebra[21]

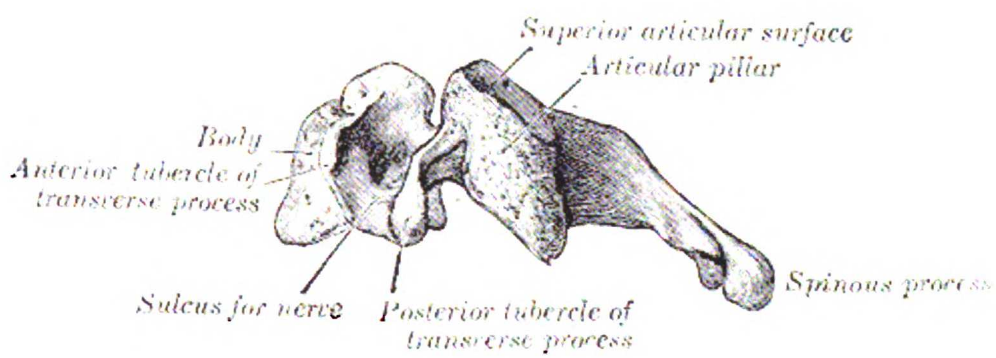

Figure 2: Schematic of a lateral aspect of a typical adult human cervical vertebra[21]

The vertebrae articulate with one another via fibrocartilaginous disks, and are connected to one another with ligaments. The large central vertebral foramen contains the spinal cord.

On a two-dimensional cephalometric radiograph as many as nine structures of the vertebrae will be superimposed on one another, making reliable identification difficult.[22]

Growth of the Cervical Vertebrae

For normal children, growth in height can be divided into several stages: constant growth until puberty, a pubertal growth spurt, slowing and eventual cessation of growth.[23] The vertebral foramen increases rapidly early in life, mostly during the first three years, and then reaches its adult size.[24,25] The morphology of the cervical vertebrae, interestingly, does not change from around the age of two years until the beginning of the growth spurt.[26,27] As the growth spurt begins, the changes that do occur are sequential and predicable. Some of these changes are demonstrated in Figure 3.

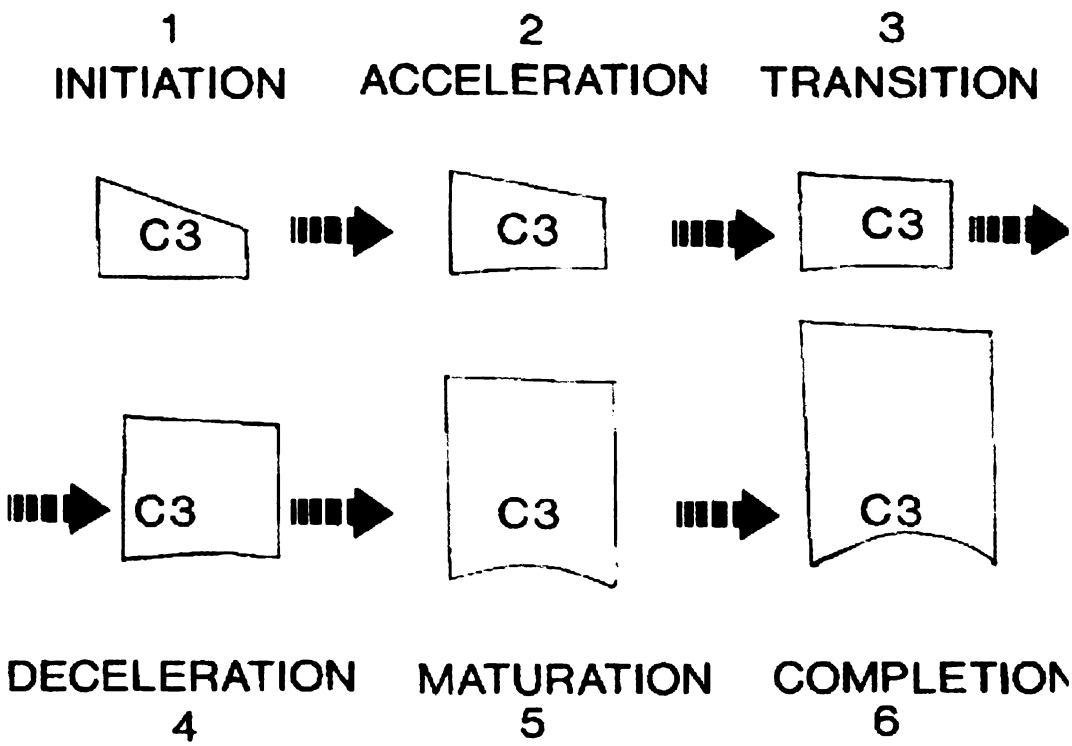

Figure 3: Sequential changes of the cervical vertebral body with growth[16]

The vertebral changes in the inferior region of the body are due to growth of epiphyseal cartilage plates, similar to the growth of long bones, whereas appositional growth, which increases vertebral height.[28] Epiphyseal growth takes place from the cartilage on both the superior and inferior surfaces of the vertebrae. Radiological analysis of vertebrae in active and paralyzed children show that the vertebrae develop the same, suggesting that the growth and development of the vertebral body is genetically determined and unaffected by mechanical factors.[25]

Progressive "cupping" of the inferior surface of the vertebral body has been the most common indicator of skeletal age cited in previous growth studies.[11] The vertebrae show this change sequentially, in descending order from C2 to C5, as the growth spurt approaches and eventually passes. Recent studies show that the vertical height of C2 increases by approximately 30 mm, and C3-C6 increase by approximately 10 mm during the growth spurt.[24,25] Figure 4 is a schematic drawing showing the average changes of C2-C4 with time.

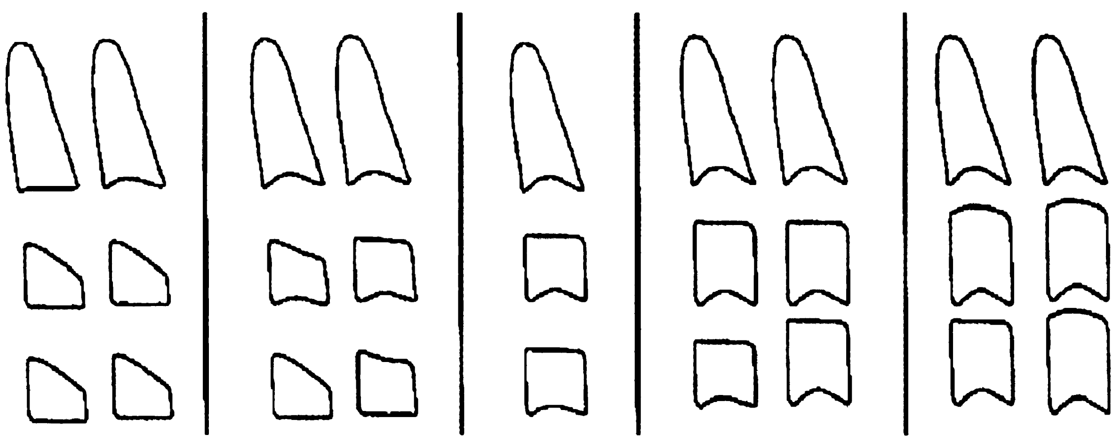

Figure 4: Changes of C2, C3, and C4 with time. The first panel from the left is before the growth spurt, the second panel is the beginning of the spurt, the third panel is the immediately following the spurt, and the remaining two are one and two years later, respectively (adapted from Baccetti, 2002).

Peak Growth Velocity and the Jaws

The pubertal growth spurt is closely correlated with the peak growth velocity.[29] Additionally, peak mandibular growth is also correlated with the pubertal growth spurt.[12,30] Therefore, it can be concluded that a cervical vertebral analysis is an effective and accurate method for predicting peak growth of the jaws, and is useful in determining the ideal time to begin orthopedic treatment.

In fact, the greatest increment in mandibular and craniofacial growth has been shown to coincide with the peak velocity in statural height.[12] This statement has been supported by several studies.[31-37] It has been further shown that the growth curves for the velocity of statural height is the most useful aid for estimating the growth potential of the mandible.[38] Figure 5 demonstrates the close relationship of the growth velocity of height and the mandible.[32]

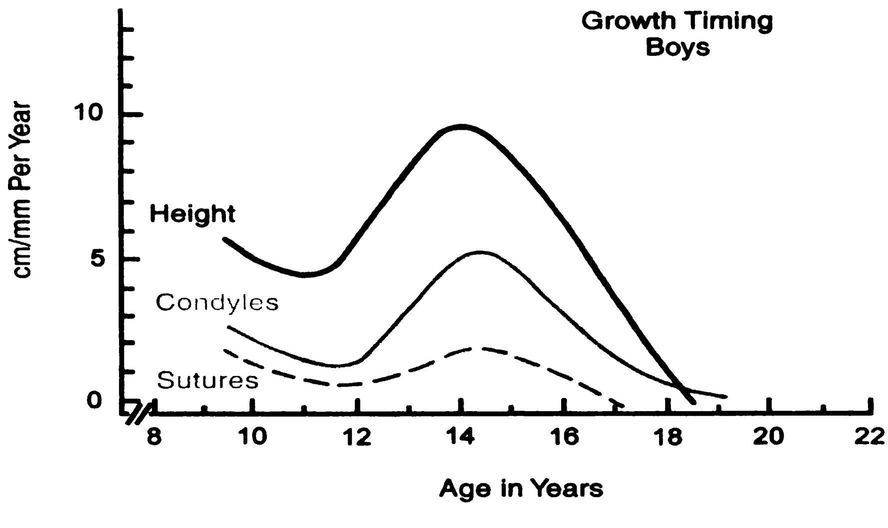

Figure 5: On average, the spurt in growth of the jaws occurs at about the same time as the peak in height (adapted from Björk, 1966[32])

The correlation of the hand-wrist to the cervical vertebrae was first described in 1972 by Lamparski.[14] The cervical vertebral maturation stages were found to be well correlated with increases in mandibular growth in 1988 by O'Reilly,[20] and was further correlated with increases in stature in 1993.[19] More recently, several methods of vertebral analysis have been shown to be very well correlated to the hand-wrist,[11,13,16] confirming the use of the cervical vertebrae for determining growth potential of the jaws and assisting in orthodontic treatment planning.

Cone-Beam Computed Tomography (CBCT)

As stated previously, in a lateral cephalogram, as many as nine structures of the vertebrae will be superimposed on one another, compromising accurate analysis.[22] Previous studies have had to accept the limitations of two-dimensional imaging, including distortion and artifacts.[39-41] However, the introduction of cone-beam computed tomography (CBCT) has vastly improved the imaging quality available to orthodontists, and has allowed for imaging of structures with minimal distortion. To visualize structures in three dimensions with minimum distortion facilitates a more accurate diagnosis.

In order to capture an image, the CBCT beam rotates around the patient and collects a volume of information.[42,43] The raw data is calculated along with additional information such as slice thickness to create voxels (3-D data points) that correspond to predefined computed attenuation coefficients, known as Hounsfield Units (HU).[44] The scale of HU is defined such that -1024 HU is the attenuation produced by air, and 0 HU is the attenuation produced by water.[45]

Adjusting the range of HU visible on an image is a powerful method for selecting specific regions or structures of interest. For example, it is possible to specifically image one vertebra in 3-D from all aspects. This would be accomplished by threshold segmenting, in which a range of HU is chosen so that only bone is visible (-200 to +500 HU) and any surrounding bone can be cut away using a software program.[45,46]

Accuracy of CBCT Imaging

Several studies have demonstrated the accuracy of CBCT imaging. Yamamoto demonstrated extremely precise spatial resolution with a tight standard deviation.[47] Araki showed that the resolution of the CBCT was extraordinarily accurate, and that images were within 99% of ideal.[48] Another study by Sukovic is in agreement.[44]

Kitaura found that measurements made on the CBCT images of a dry skull were within 2% of those made on the actual skull itself.[49] Another study by Matteson placed radio-opaque markers on a dry skull, took conventional 2-D lateral cephalograms and a CT image, and found that the accuracy of the CT was consistently greater.[50]

CBCT imaging is an invaluable tool for visualizing the underlying structures of patients because it gives a full, accurate, and minimally distorted view. Software improves visualization of anatomy and allows orthodontists to better understand and treat their patients.

Purpose of the Present Study

Being aware of the limitations and inaccuracies of traditional two-dimensional imaging, I propose to develop a reliable method of measuring landmarks on and to study the vertebral morphology of the cervical vertebrae using 3-D CBCT and correlate findings with age.

Specific Aims

The specific aims are to conduct a retrospective, cross-sectional study and:

1. Accurately separate a 3-D rendering of the cervical vertebrae from a CBCT scan
2. Identify useful landmarks
3. Correlate vertebral morphology to the patient's skeletal age
4. Assess the reproducibility of a 3-D analysis

Null Hypothesis

There is no correlation between the 3-D measurements of the cervical vertebrae and age.

Methods

This was a cross-sectional, retrospective study of twenty-three patients. Patients were randomly selected for study from a CBCT database managed by the University of California San Francisco (UCSF) Craniofacial Imaging Center. Patients varied in age from 7 to 17 years old. The patients were selected based on the following criteria:

Inclusion Criteria

- Patients have a clear CBCT image which has captured cervical vertebrae 3, 4, and 5

- Informed consent obtained from patient for use in research (CHR # H893-23246-02)

Exclusion Criteria

- Patients are no more than 17 years of age
- Patients have no craniofacial anomalies or obvious cranioskeletal asymmetries

Image Acquisition & Processing

The patient images were captured at UCSF using the Hitachi MercuRay® CBCT (Hitachi Medical Corp, Tokyo, Japan) with parameters of 120 kVp, 15mA, a 0.376 mm slice thickness, and a total of 512 slices in DICOM format.

The third, fourth, and fifth cervical vertebrae (C3, C4, C5) of each subject were segmented from the three dimensional image by one of three examiners (GM, an orthodontic resident; LH and TC, two dental students) using the CB Works 2.1 software (CyberMed, Seoul, Korea) in DICOM format. The vertebrae were threshold segmented by selecting appropriate thresholds of Hounsfield Units (HU), and isolated by digitally sculpting away any extraneous hard and soft tissue using the segmentation tool in CB Works, and then adjusting the range of visible HU to allow for further sculpting of previously unseen data (noise). In order to properly threshold segment, a range of HU must be selected that includes the material of interest. Specifically, bone falls in the -200 HU to +500 HU range. To minimize error, the image was rotated so as to be viewed in all three planes of space to determine whether visualized structures were, in fact, part of the object or noise. A minimal amount of noise remained for each vertebra, providing an accurate three-dimensional surface and volume model which could be saved in the VRML format to export.

Data Points

After the vertebrae were isolated, the data were transferred to the Amira 3.1® software (Mercury Computer Systems, Chelmsford, MA) as a VRML (.wrl) file. The resulting set of voxels was transformed by the software into a 3-D surface mesh. The surface quality was set at high. A surface area map was generated as a hexadecimal binary surface (.surf) with unconstrained smoothing, high surface quality, and a critical surface angle of 120°. This helped eliminate the "stair-step" artifacts due to the borders of the tetrahedral mesh, at the expense of rendering larger data files. The data were analyzed by one examiner (GM). Linear and angular measurements were taken using the "Measuring tool" in Amira.

Fourteen landmarks were chosen for measurement (Table 1).

Table 1: Landmarks chosen for measurement

Abbreviation	Description
Bas	Most anterior-superior point of the vertebral body
Bps	Most posterior-superior point of the vertebral body
Bai	Most anterior-inferior point of the vertebral body
Bpi	Most posterior-inferior point of the vertebral body
Bsl	Most superior-lateral part of the vertebral body (left)
Bsr	Most superior-lateral part of the vertebral body (right)
Bil	Most inferior-lateral part of the vertebral body (left)
Bir	Most inferior-lateral part of the vertebral body (right)
Bs	Center of the vertebral body (superior surface)
Bi	Center of the vertebral body (inferior surface)
La	Most anterior point of the vertebrae within the lumen
Lp	Most posterior point of the vertebrae within the lumen
Ll	Most lateral point of the vertebrae within the lumen (left)
Lr	Most lateral point of the vertebrae within the lumen (right)

All points were chosen based on the judgment of one examiner (GM). Four points were chosen on the superior surface of the body (anterior, posterior, left, and right). Each point was placed at the most convex point on the curve from the superior portion of the body to the corresponding vertical wall (Figure 6). One additional point was chosen at the most inferior portion of the superior surface of the body if it was concave, or the most superior portion of the body if it was convex. Five corresponding points were selected on the inferior surface of the body in the same manner. Within the lumen of the vertebrae, four additional points were chosen. These points were located in the superior-inferior center of the lumen of the vertebrae, one each at the most anterior, posterior, left, and right internal surfaces.

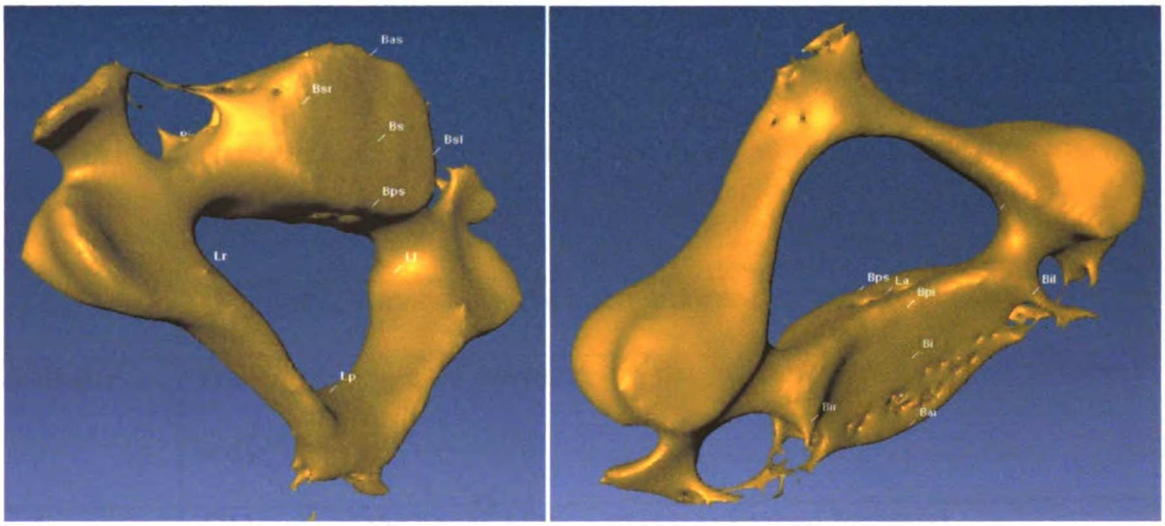

Figure 6: Points chosen for measurement on the vertebral body.

Measurements

Four angular and six linear measurements were taken on each vertebra using the defined landmarks (Table 2).

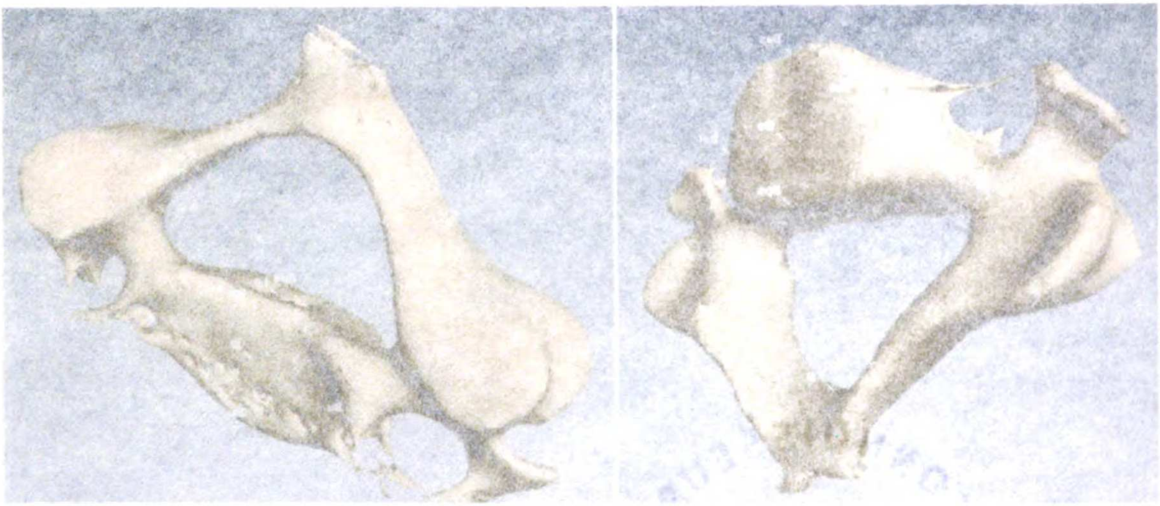

Table 2: Measurements taken on each vertebra

Abbreviation	Description
Bas-Bai	Height of the anterior portion of the vertebral body
Bps-Bpi	Height of the posterior portion of the vertebral body
Bas-Bps	AP length of the superior portion of the vertebral body
Bai-Bpi	AP length of the inferior portion of the vertebral body
Bas-Bs-Bps	AP angle of curvature of the superior portion of the vertebral body
Bsl-Bs-Bsr	Transverse angle of curvature of the superior portion of the vertebral body
Bai-Bi-Bpi	AP angle of curvature of the inferior portion of the vertebral body
Bil-Bi-Bir	Transverse angle of curvature of the inferior portion of the vertebral body
La-Lp	AP length of the lumen of the vertebra (vertebral foramen)
Ll-Lr	Transverse length of the lumen of the vertebra

Each linear measurement was defined as the distance between two points (Figure 7).

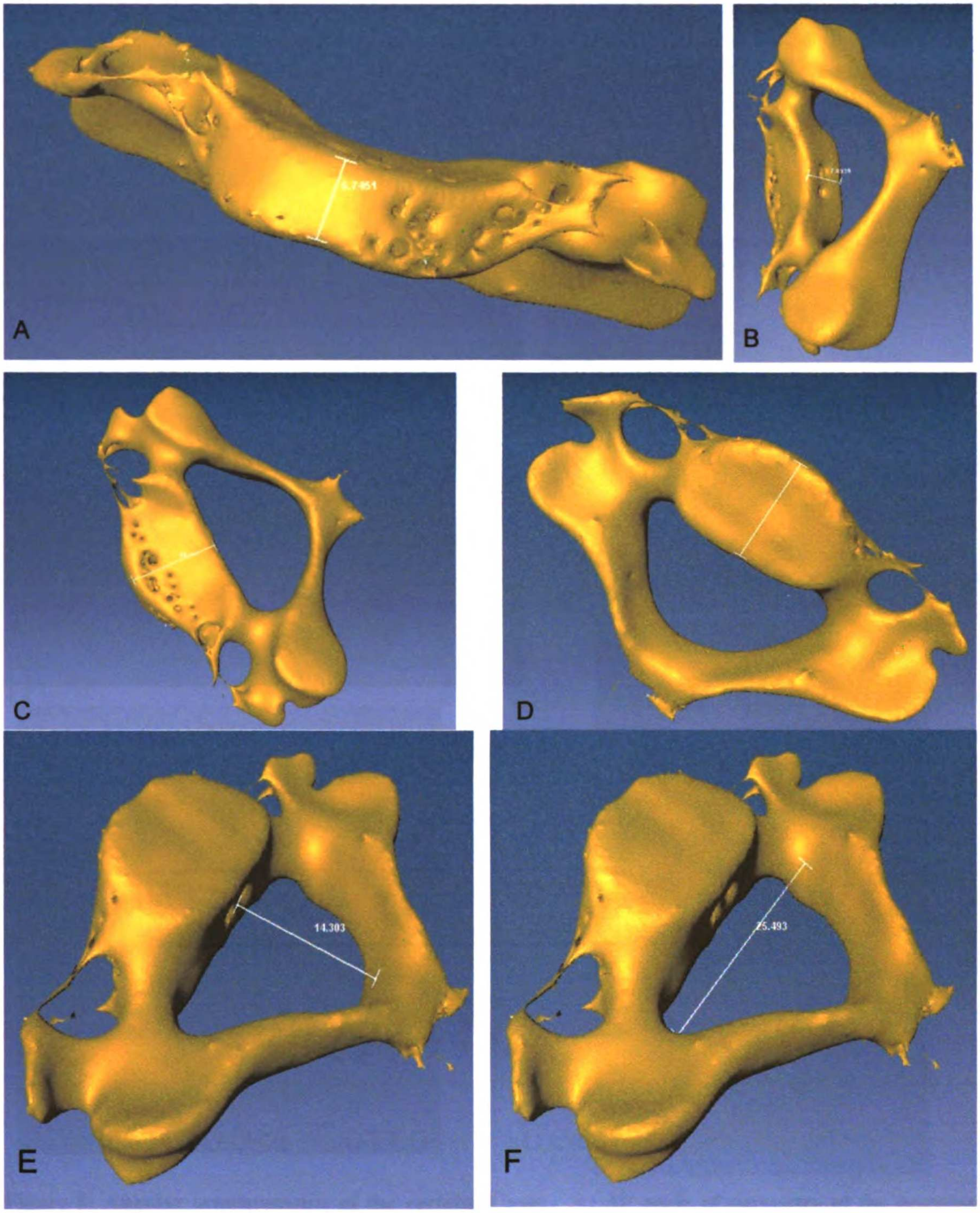

Figure 7: Linear measurements of the vertebral body. A: Height of the anterior portion of the vertebral body (Bas-Bai); B: Height of the posterior portion of the vertebral body (Bps-Bpi); C: AP length of the superior portion of the vertebral body (Bas-Bps); D: AP length of the inferior portion of the vertebral body (Bai-Bpi); E: AP length of the vertebral foramen (La-Lp); F: Transverse length of the vertebral foramen (Ll-Lr).

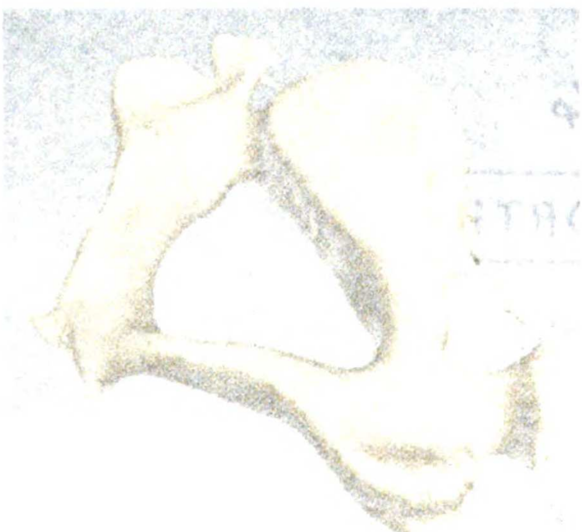

In addition, the angular measurement was defined as the angle formed by three points, where a concave measurement was assigned a value less than 180°, and a convex measurement greater than 180° (Figure 8).

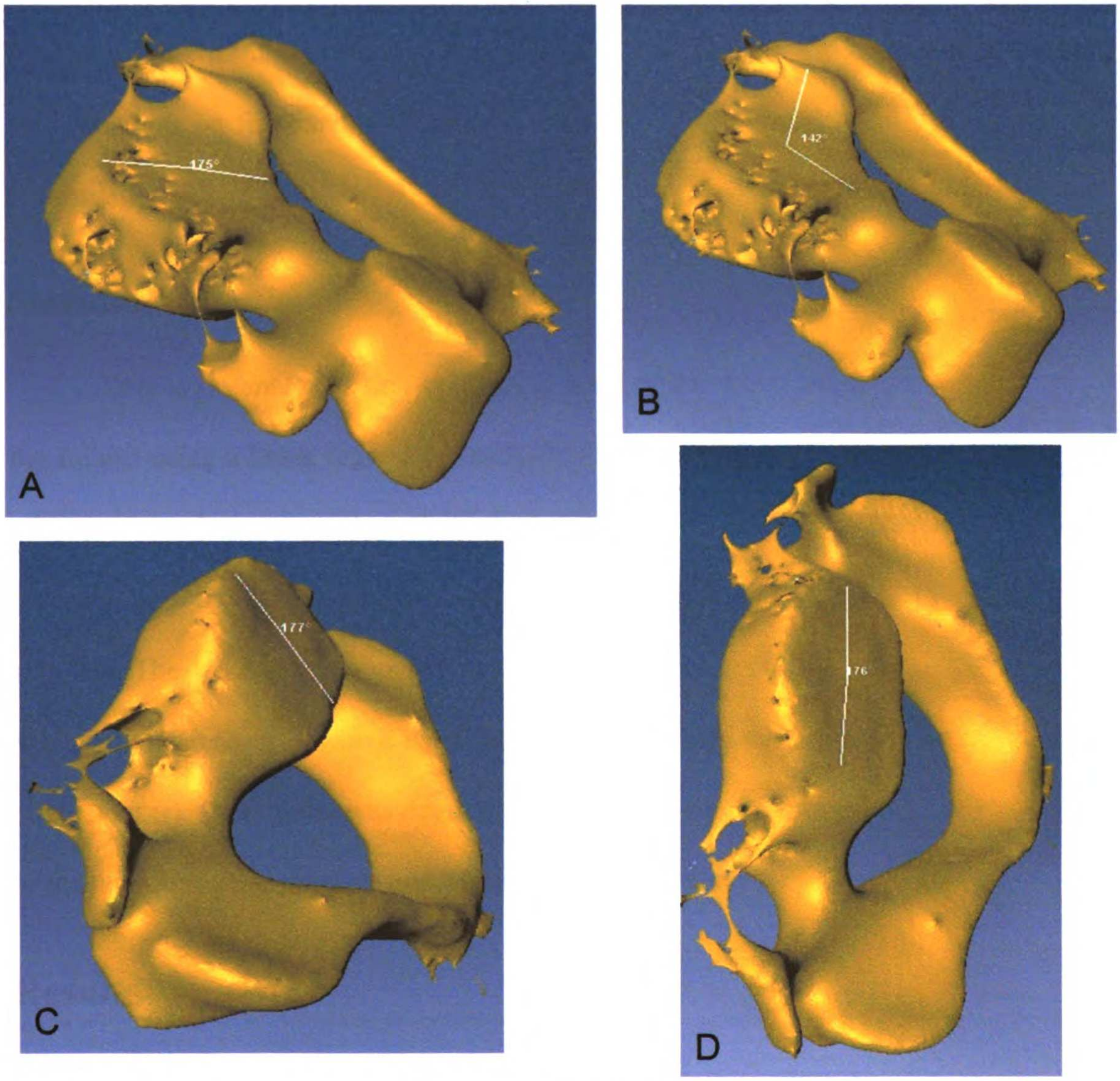

Figure 8: Angular measurements of the vertebral body. A: AP angle of curvature of the superior portion of the vertebral body (Bas-Bs-Bps); B: Transverse angle of curvature of the superior portion of the vertebral body (Bsl-Bs-Bsr); C: AP angle of curvature of the inferior portion of the vertebral body (Bai-Bi-Bpi); D: Transverse angle of curvature of the inferior portion of the vertebral body (Bil-Bi-Bir).

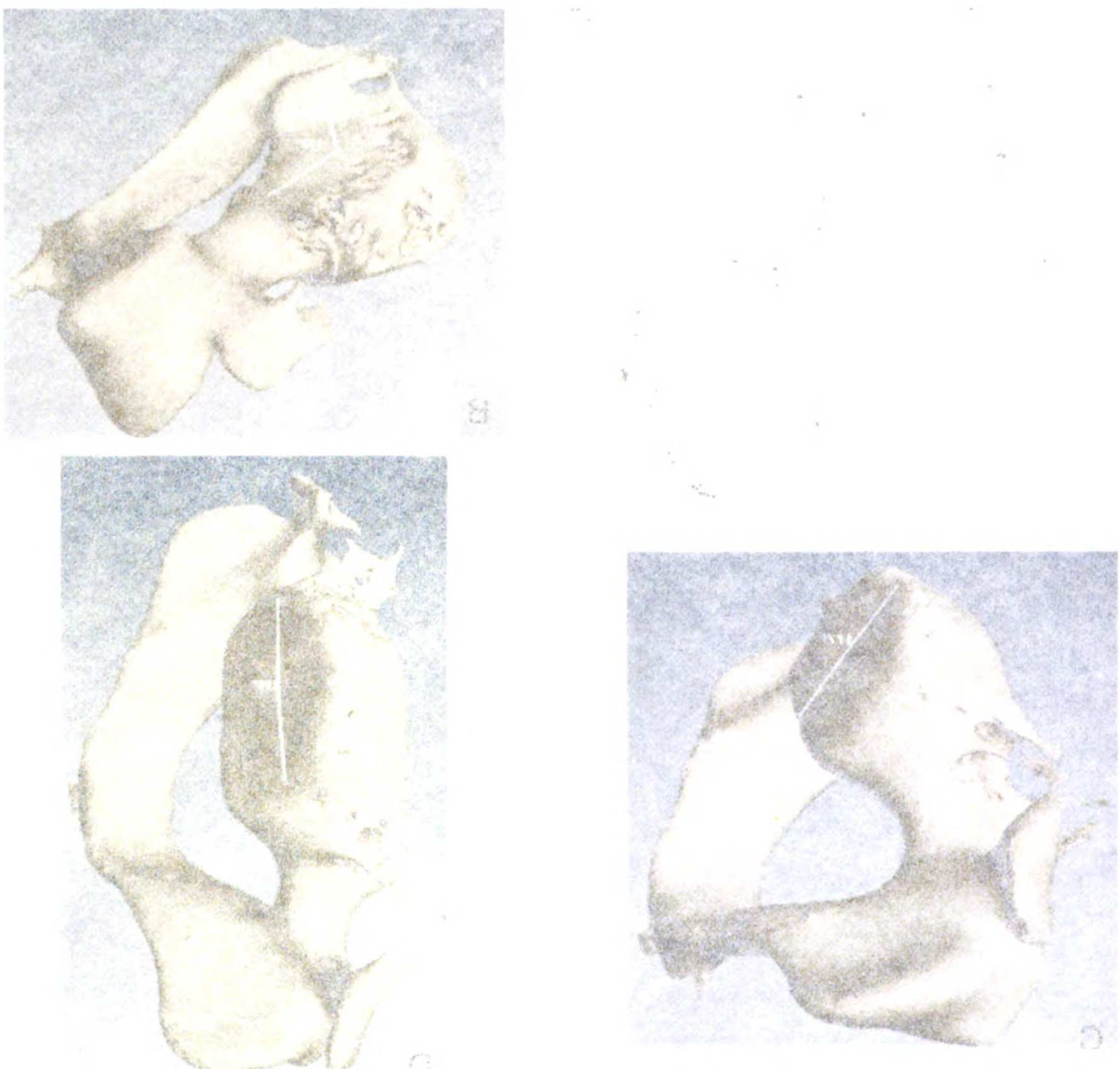

Error Measurements

Data from five patients were analyzed twice to determine reliability. Inter- and intra-operator error in sculpting was evaluated by having the primary operator (GM) re-segment five vertebrae and repeat the measurements, then compare the quality of the segmentation. Intra-operator error in landmark selection was evaluated by repeating measurements on five randomly selected subjects. This was analyzed by using a Lin's concordance test.

Statistical Analysis

Data were analyzed first comparing each of the ten measurements to the age of the subject using a linear regression analysis with a $P < 0.05$ for significance. A measure of central tendency was then delineated by the mean ± 1 SD for each of the ten measurements to indicate which measures had the smallest and largest variability in the sample. The ten measurements were then compared to each other in a simple linear regression to determine which were most correlated with each other using a correlation coefficient (r). A formula was developed based on a stepwise regression to define which of the measures were most related to the age of the subject.

Results

Error of the Method

Intra-observer measurements were taken by randomly selecting five patients and having one examiner (GM) measure each variable on each vertebra four weeks later. The majority of the measurements showed an extremely high correlation, indicating a high level of reliability of the data (Table 3).

Table 3: Intra-observer reliability

PREDICTOR	PEARSON COEFFICIENT	PEARSON PROBABILITY
C3 Anterior Body Vertical	0.99994	<.0001
C3 Inner Lumen AP	0.96179	0.0382
C3 Inner Lumen Transverse	0.89993	0.1001
C3 Lower Angle AP	0.93861	0.0614
C3 Lower Angle Transverse	0.97373	0.0263
C3 Posterior Body Vertical	0.99604	0.0040
C3 Upper Angle AP	0.56305	0.4369
C3 Upper Angle Transverse	0.73860	0.2614
C3 Lower AP Distance	0.67533	0.3247
C3 Upper AP Distance	0.92486	0.0751
C4 Anterior Body Vertical	0.96763	0.0070
C4 Inner Lumen AP	0.88940	0.0434
C4 Inner Lumen Transverse	0.30980	0.6120
C4 Lower Angle AP	0.98205	0.0029
C4 Lower Angle Transverse	0.80152	0.1029
C4 Posterior Body Vertical	0.98123	0.0031
C4 Upper Angle AP	0.97236	0.0055
C4 Upper Angle Transverse	0.97177	0.0057
C4 Lower AP Distance	0.98273	0.0027
C4 Upper AP Distance	0.99780	0.0001
C5 Anterior Body Vertical	0.94480	0.0154
C5 Inner Lumen AP	0.78551	0.1153
C5 Inner Lumen Transverse	0.88753	0.0445
C5 Lower Angle AP	0.99476	0.0005
C5 Lower Angle Transverse	0.89080	0.0426
C5 Posterior Body Vertical	0.94590	0.0150
C5 Upper Angle AP	0.92560	0.0241
C5 Upper Angle Transverse	0.78992	0.1119
C5 Lower AP Distance	0.95173	0.0126

Six of the thirty measurements have a relatively low intra-rater correlation. However, none of the differences for these six measurements are statistically significant. Furthermore, the actual millimeter and degree measurement differences for these landmarks is small and not clinically significant (Appendix A).

Descriptive Statistics

The average age for all twenty-three subjects in this study was 13.4 years (SD 2.9 years), with 14 females (mean age 13.4 years) and 9 males (mean age 13.0 years). Data for all patients are summarized in Appendices A and C.

The following figures demonstrate the relationships of the variables to age (months).

It is apparent visually that in all three vertebrae, as the patients are older there is an increased height of the anterior vertical body (Figure 9). As is evident on the scattergram, the data appear to be tight since the colored dots are all in close proximity, indicating that this same pattern exists between each patient and each vertebra. This height change appears to not be gradual, but to show a sudden shift around 12 years of age (Figure 10).

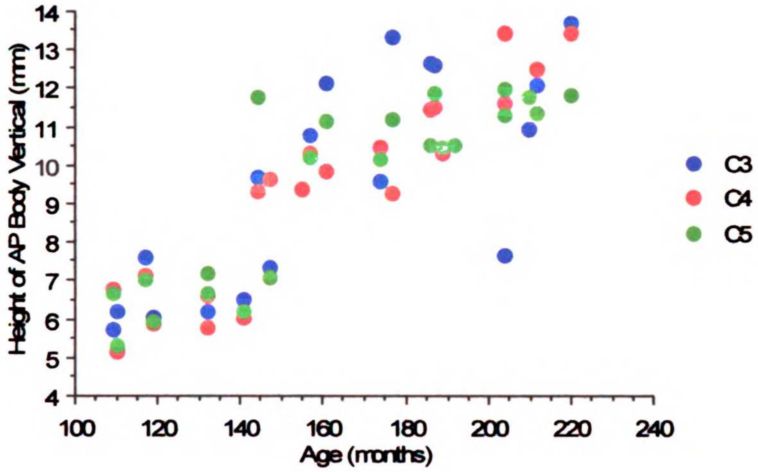

Figure 9: Height of Anterior Body Vertical vs. Age of C3, C4, C5

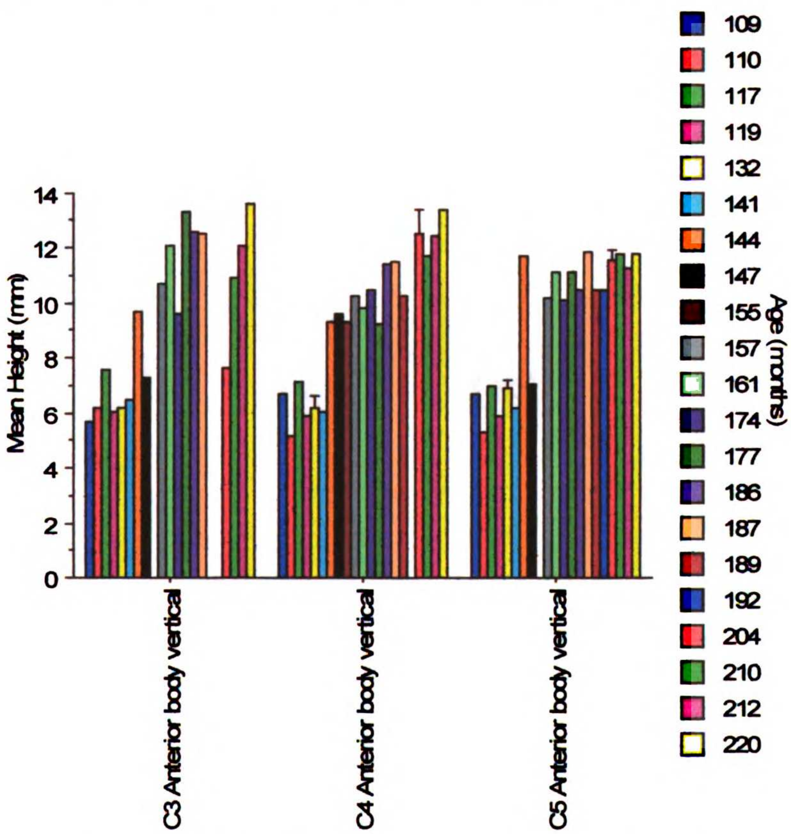

Figure 10: Bar chart of AP Body Vertical. Error Bars ±1 SEM.

The posterior height of each of the vertebrae shows a similar pattern as the anterior height, albeit less pronounced (Figures 11 and 12).

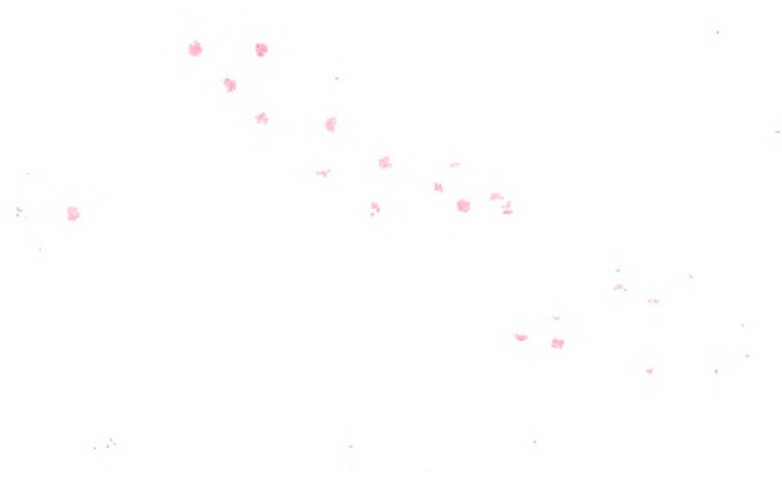

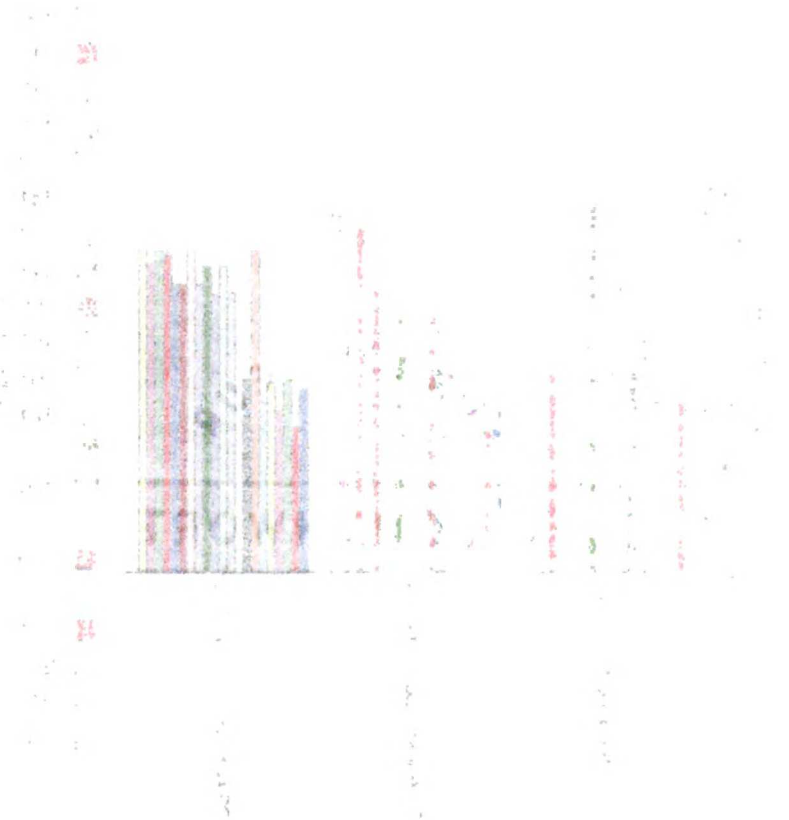

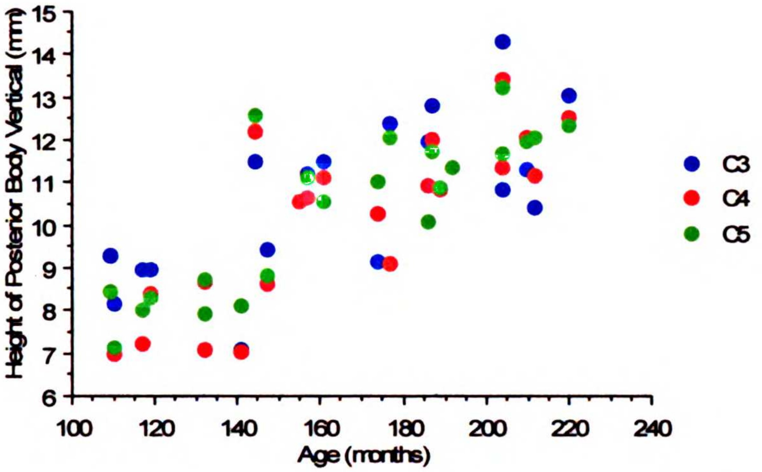

Figure 11: Height of Posterior Body Vertical vs. Age of C3, C4, C5

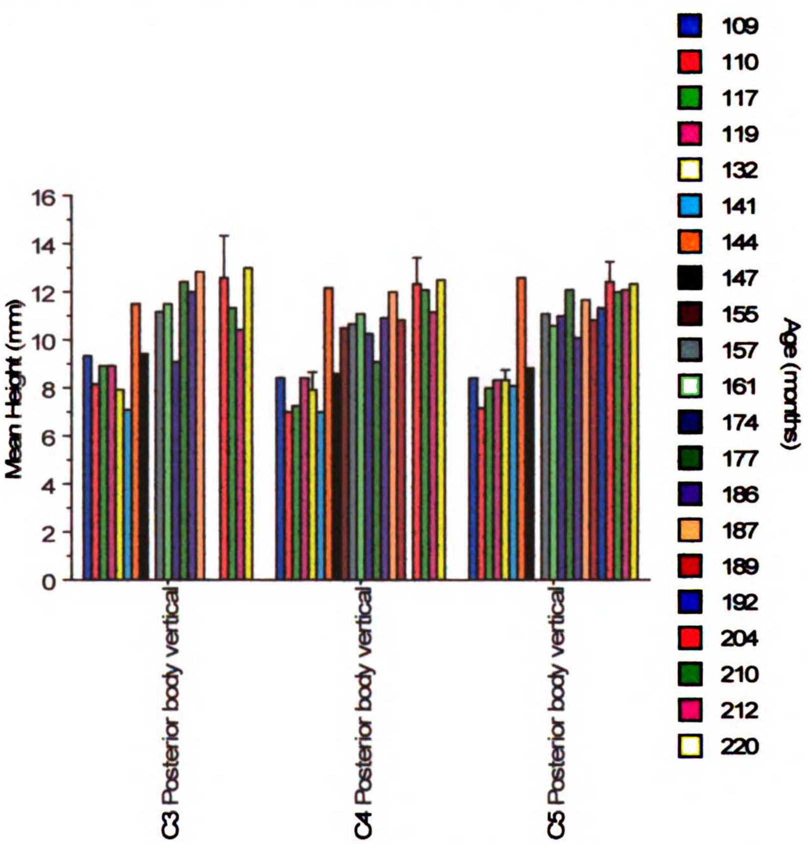

Figure 12: Bar chart of Posterior Body Vertical. Error Bars ±1 SEM.

The upper and the lower AP distance measurements demonstrate no obvious pattern with age (Figures 13-16).

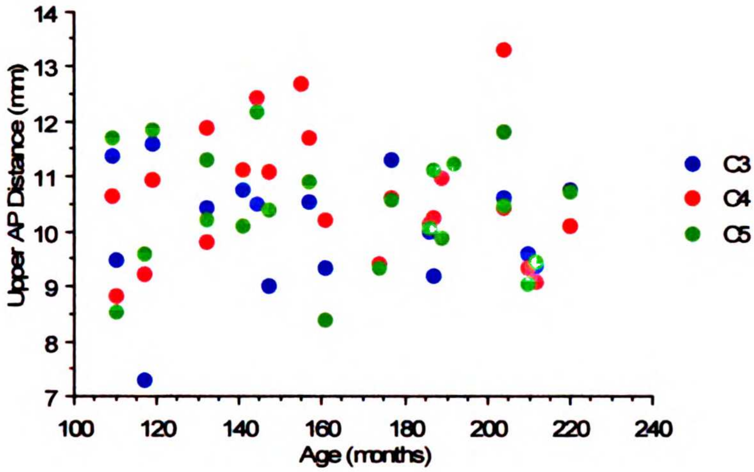

Figure 13: Upper AP Distance vs. Age of C3, C4, C5

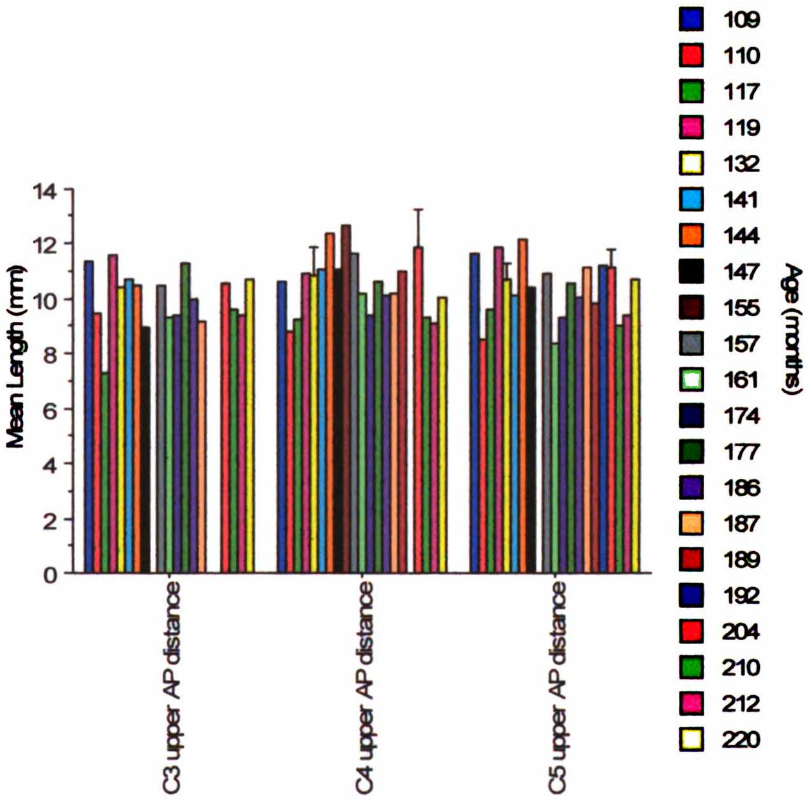

Figure 14: Bar chart of Upper AP Distance. Error Bars ±1 SEM.

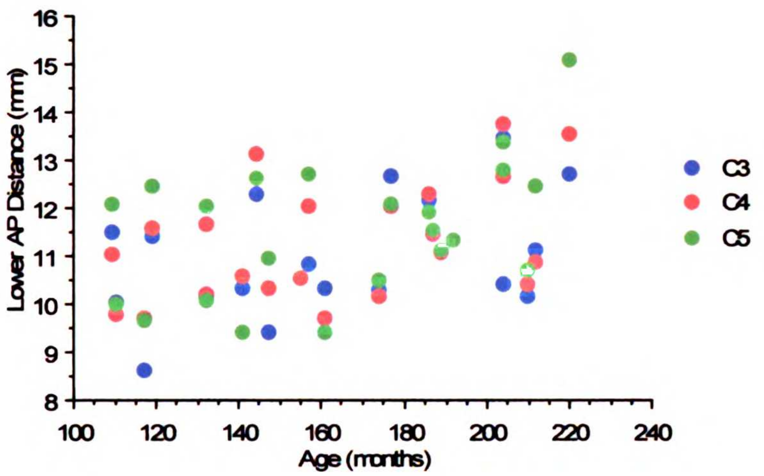

Figure 15: Lower AP Distance vs. Age of C3, C4, C5

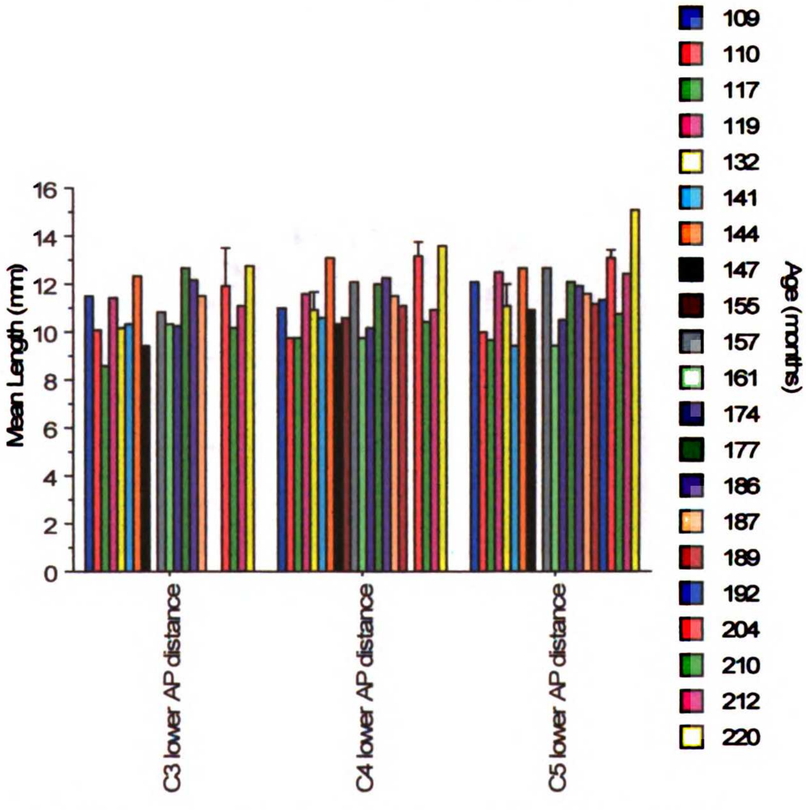

Figure 16: Bar chart of Lower AP Distance. Error Bars ±1 SEM.

The upper AP angular measurements demonstrate a slight increase in concavity with age, more so with the C5 vertebra than with C3 or C4 (Figure 17). As demonstrated previously, there appears to be a sudden change in C5 around age 12 (Figure 18).

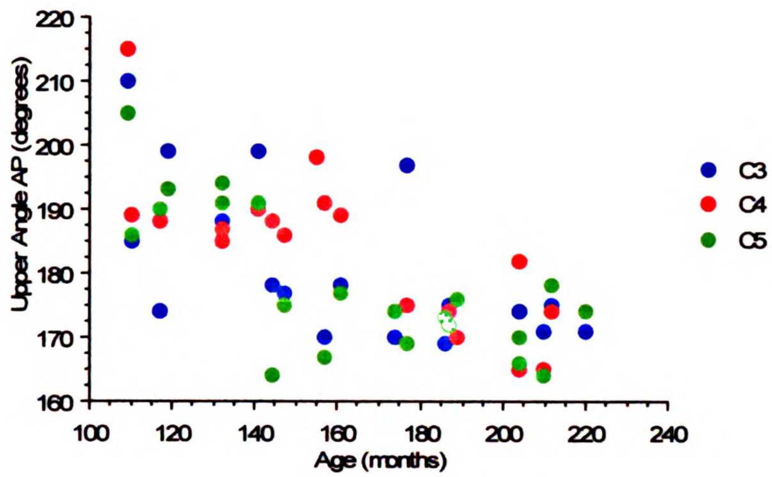

Figure 17: Upper Angle AP vs. Age of C3, C4, C5

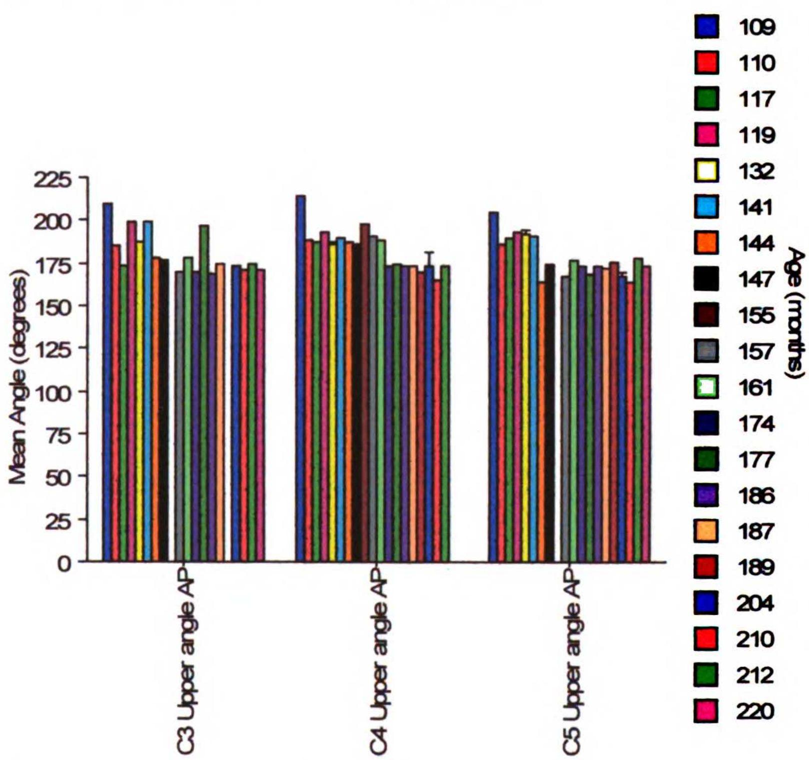

Figure 18: Bar chart of Upper Angle AP. Error Bars ±1 SEM.

The upper transverse angle measurements show no obvious pattern with age in any of the vertebrae measured (Figures 19 and 20).

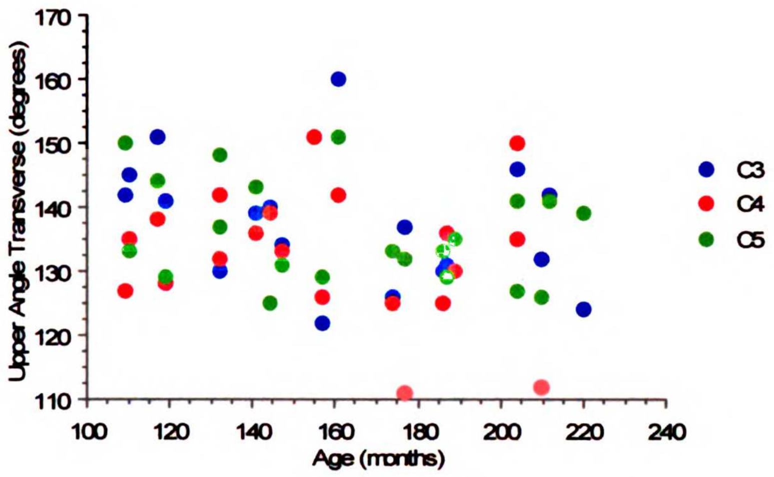

Figure 19: Upper Angle Transverse vs. Age of C3, C4, C5

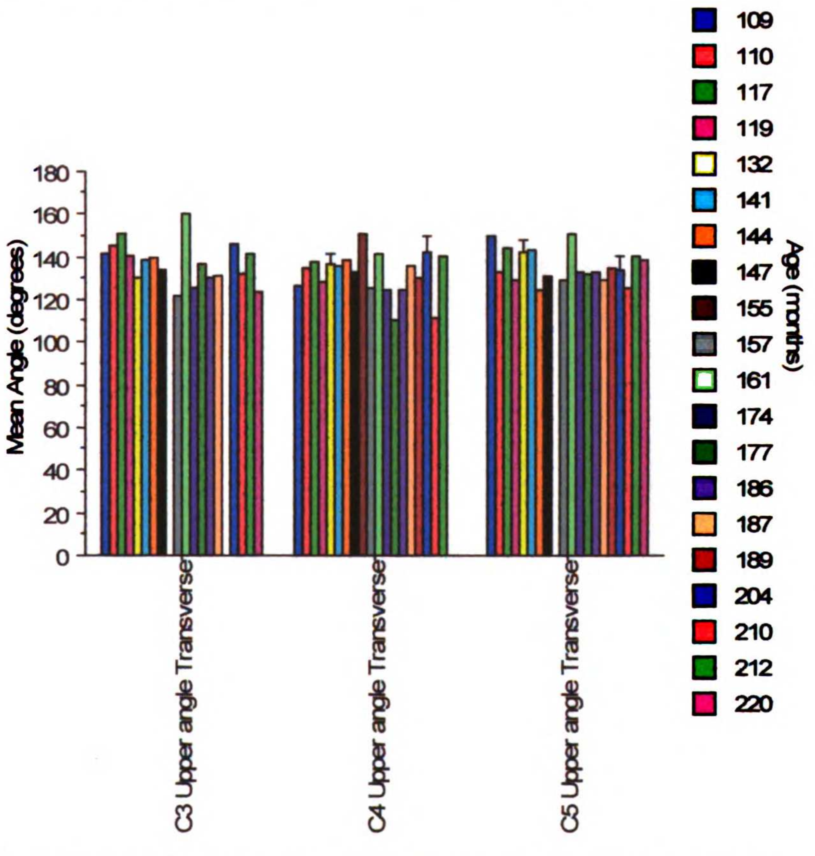

Figure 20: Bar chart of Upper Angle Transverse. Error Bars ±1 SEM.

The lower angle AP shows readily demonstrable increase in concavity with age (Figure 21). This appears to gradually and smoothly change with age (Figure 22).

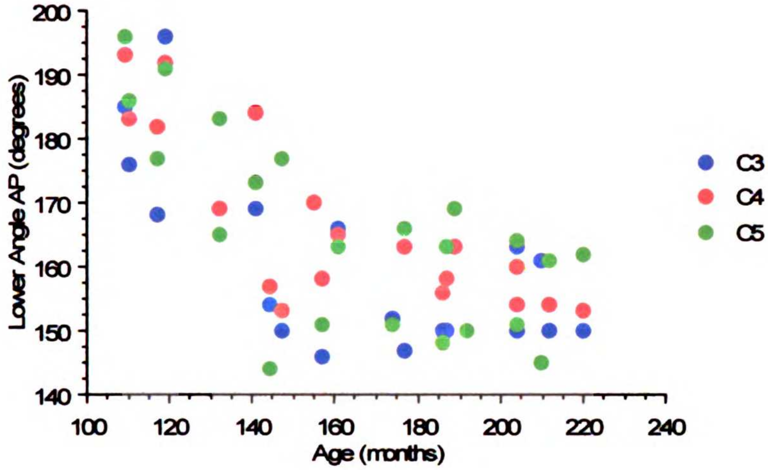

Figure 21: Lower Angle AP vs. Age of C3, C4, C5

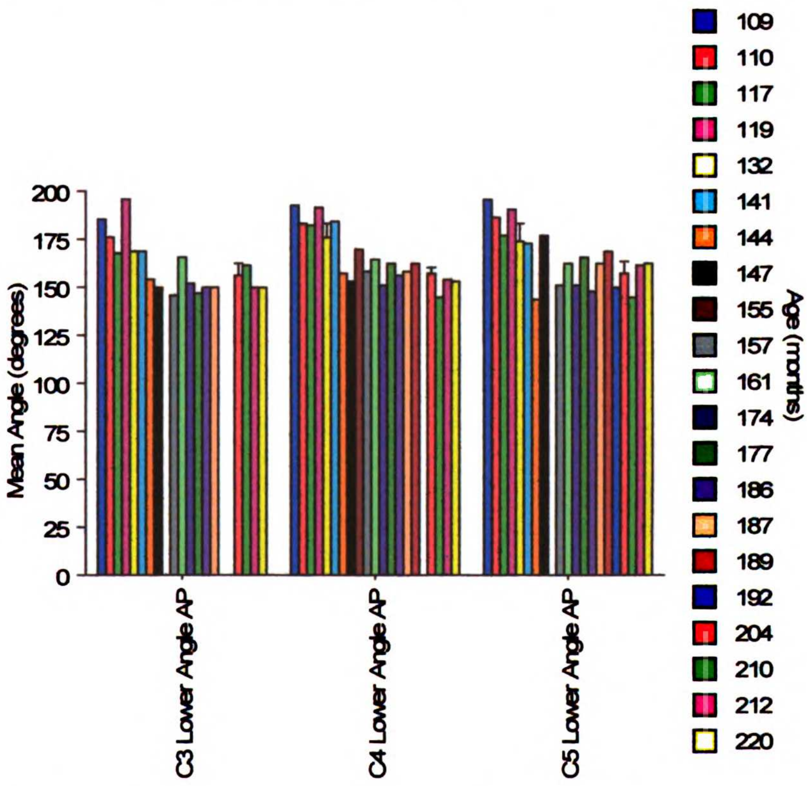

Figure 22: Bar chart of Lower Angle AP. Error Bars ±1 SEM.

As with the upper transverse measurements, the lower transverse measurements do not clearly demonstrate any changes with age (Figures 23 and 24).

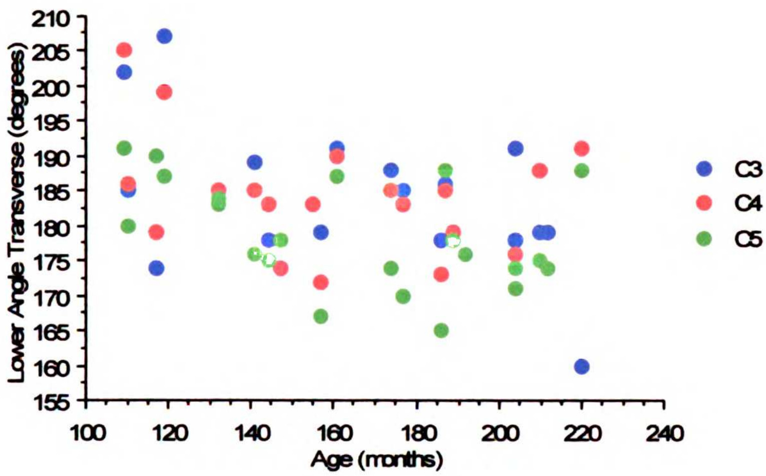

Figure 23: Lower Angle Transverse vs. Age of C3, C4, C5

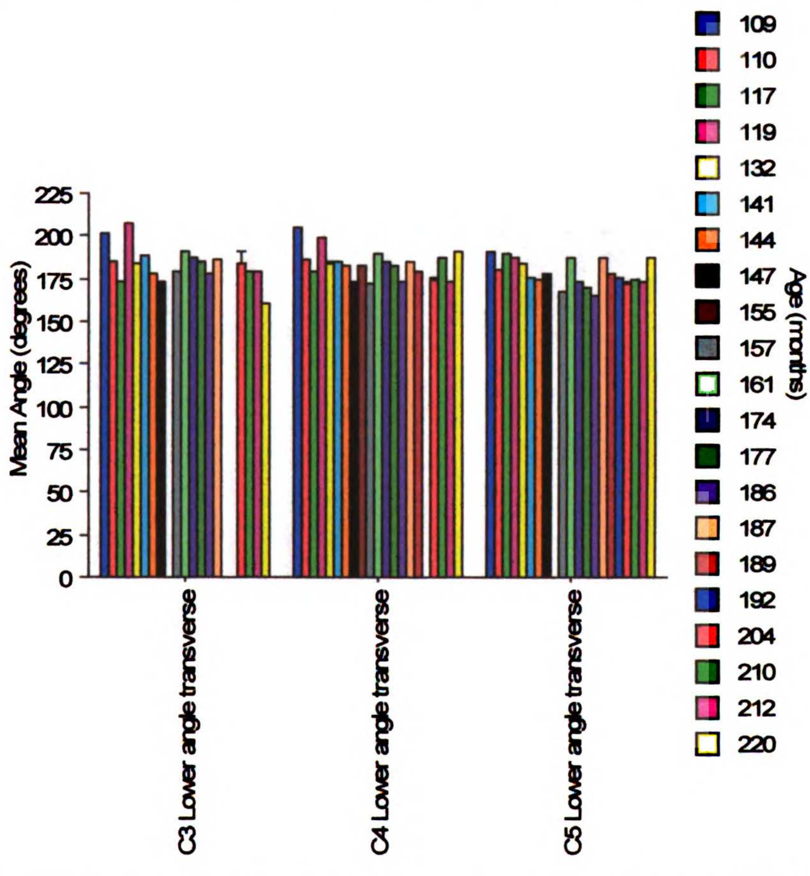

Figure 24: Bar chart of Lower Angle Transverse. Error Bars ±1 SEM.

The inner lumen AP shows no obvious pattern with age (Figures 25 and 26). Interestingly, the inner lumen transverse appears to vary little between any of the vertebrae in any aged patient (Figures 27 and 28).

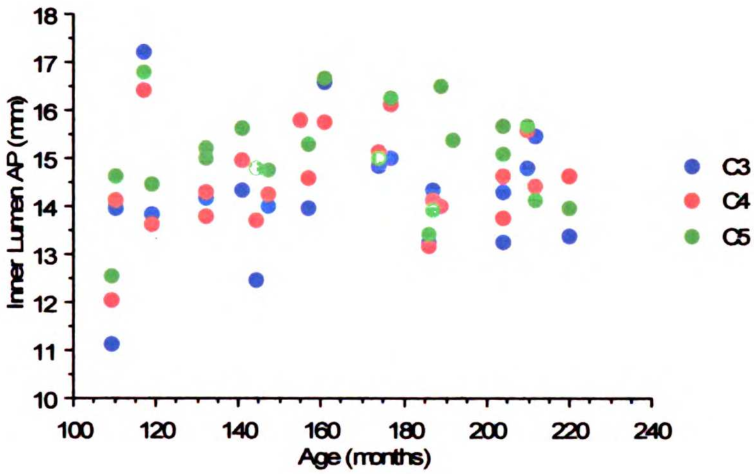

Figure 25: Inner Lumen AP vs. Age of C3, C4, C5

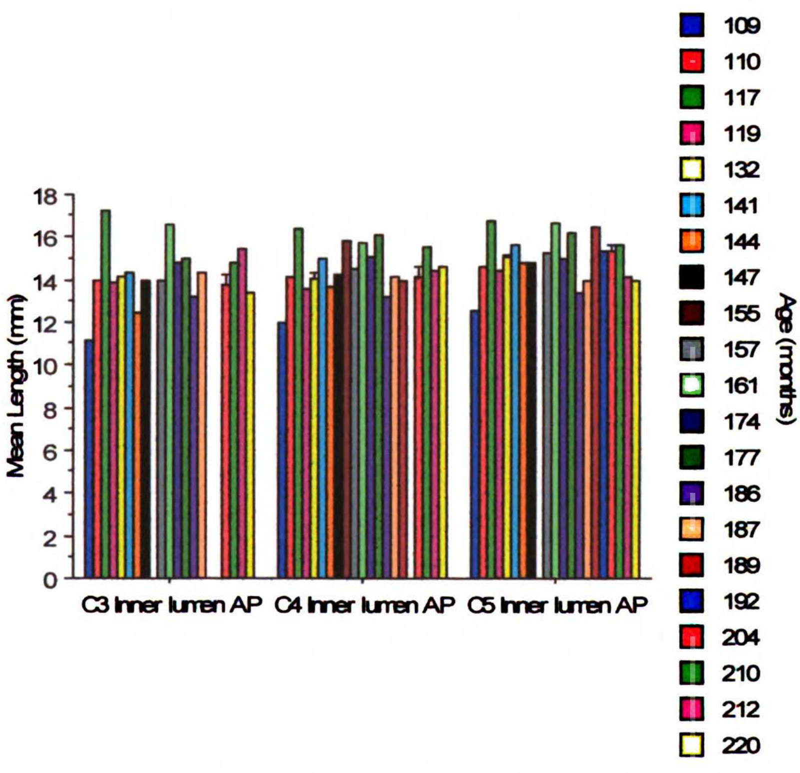

Figure 26: Bar chart of Inner Lumen AP. Error Bars ±1 SEM.

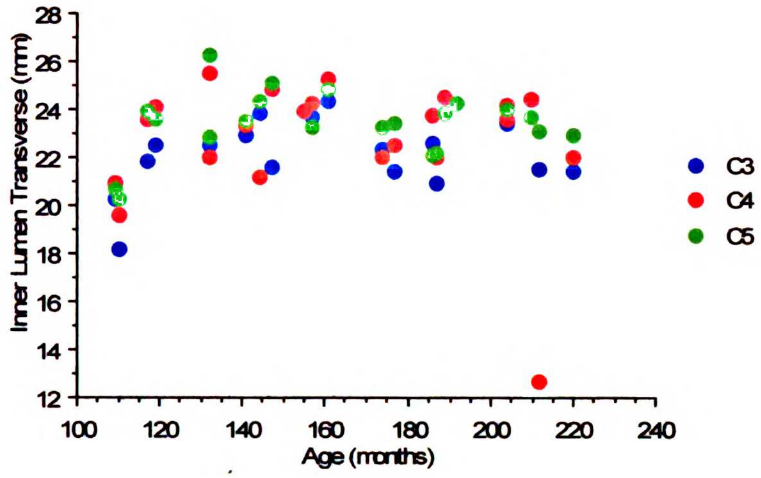

Figure 27: Inner Lumen Transverse vs. Age of C3, C4, C5

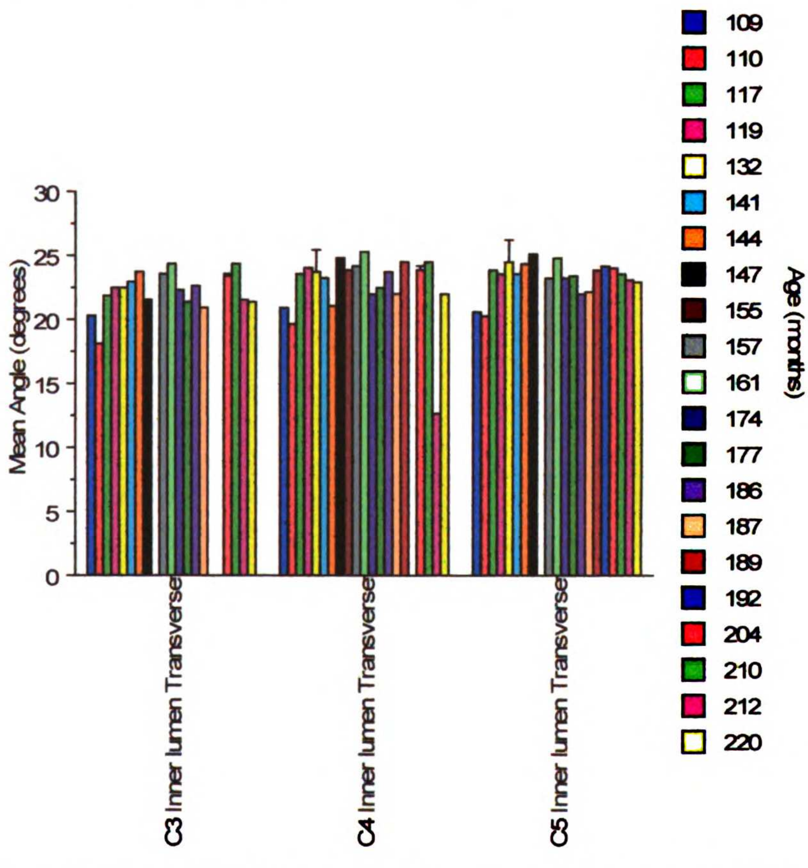

Figure 28: Bar chart of Inner Lumen Transverse. Error Bars ±1 SEM.

Correlation of Morphology to Age

There were several significant morphological measurements that were correlated with age on all three vertebrae (Table 4). Interestingly, gender differences were not significant.

Table 4: Correlation of morphology to age (months)

Variable	N	Pearson Correlation	Pearson p-value	Pearson 95% CI Lower	Pearson 95% CI Upper
C4 Anterior Body Vertical	22	0.93	<.0001	0.83	0.97
C5 Anterior Body Vertical	22	0.86	<.0001	0.69	0.94
C5 Posterior Body Vertical	22	0.84	<.0001	0.66	0.93
C4 Posterior Body Vertical	22	0.81	<.0001	0.59	0.92
C3 Anterior Body Vertical	18	0.77	0.0002	0.47	0.91
C3 Posterior Body Vertical	19	0.72	0.0006	0.39	0.88
C4 Lower AP Distance	22	0.46	0.0296	0.05	0.74
C5 Lower AP Distance	22	0.45	0.0344	0.04	0.73
C5 Lower Angle Transverse	22	-0.43	0.0445	-0.72	-0.01
C3 Lower Angle Transverse	19	-0.47	0.0439	-0.76	-0.02
C3 Upper Angle AP	18	-0.6	0.0088	-0.83	-0.18
C3 Lower Angle AP	19	-0.68	0.0013	-0.87	-0.33
C5 Lower Angle AP	22	-0.69	0.0004	-0.86	-0.37
C5 Upper Angle AP	21	-0.73	0.0002	-0.88	-0.44
C4 Upper Angle AP	21	-0.8	<.0001	-0.91	-0.56
C4 Lower Angle AP	22	-0.82	<.0001	-0.92	-0.6

The strongest correlations between age and morphology were in the anterior and posterior vertical body height, and the lower and upper AP angles of all three vertebrae.

Prediction Models

In order to develop a clinically relevant application, a predictive model equation was developed, based on the morphological characteristics noted at the time of scan, corresponding to the approximate skeletal age. A regression analysis using SAS Version 9.1 (SAS Institute, Cary, NC) was used to build a model which predicts age using vertebral measurements.

The vertebrae measurements were considered on their original scale and two transformed scales. The measurements were log-transformed. Within C3, C4, and C5, the log Inner Lumen AP was subtracted from each of the other log transformed measurements. Since neural tissue, and therefore the spinal cord, does not change size significantly after age 6, this would be a logically stable measurement.[51]

The following correlations were computed: 1) correlations of untransformed vertebral variables within themselves plus age (Table 5); 2) correlations of log transformed vertebral variables within themselves plus age (Table 6); and 3) correlations of log vertebral difference variables within themselves plus age plus log(Inner Lumen AP) (Table 7).

Table 5: Correlation of log measurements of morphology to age (months)

Variable	n	Pearson Correlation	Pearson p-value	Pearson 95% CI Lower	Pearson 95% CI Upper
LOG C4 Anterior Body Vertical	22	0.91	<.0001	0.78	0.96
LOG C5 Anterior Body Vertical	22	0.86	<.0001	0.68	0.94
LOG C5 Posterior Body Vertical	22	0.85	<.0001	0.67	0.94
LOG C4 Posterior Body Vertical	22	0.81	<.0001	0.58	0.92
LOG C3 Anterior Body Vertical	18	0.78	0.0001	0.49	0.91
LOG C3 Posterior Body Vertical	19	0.71	0.0006	0.38	0.88
LOG C4 Lower AP Distance	22	0.46	0.0304	0.05	0.74
LOG C5 Lower AP Distance	22	0.45	0.0368	0.03	0.73
LOG C5 Lower Angle Transverse	22	-0.43	0.0454	-0.72	-0.01
LOG C3 Lower Angle Transverse	19	-0.46	0.045	-0.76	-0.01
LOG C3 Upper Angle AP	18	-0.6	0.0082	-0.83	-0.19
LOG C5 Lower Angle AP	22	-0.67	0.0006	-0.85	-0.35
LOG C3 Lower Angle AP	19	-0.68	0.0013	-0.87	-0.33
LOG C5 Upper Angle AP	21	-0.73	0.0002	-0.88	-0.43
LOG C4 Upper Angle AP	21	-0.81	<.0001	-0.92	-0.57
LOG C4 Lower Angle AP	22	-0.82	<.0001	-0.92	-0.6

Analyzing the log transformed vertebral variables demonstrates that the highest correlations to age include the vertical height of all three vertebral bodies, as well as the upper and lower AP angles. The strongest correlations exist, in decreasing order with: C4 anterior body vertical, C5 anterior body vertical, C5 posterior body vertical, C4 lower angle AP, C4 upper angle AP, and C4 posterior body vertical.

Table 6: Correlation of log measurements subtracted from log inner lumen AP to age (months)

Log variable subtracted from Log Inner Lumen AP	N	Pearson Correlation	Pearson p-value	Pearson 95% CI Lower	Pearson 95% CI Upper
C4 Anterior Body Vertical	22	0.86	<.0001	0.69	0.94
C5 Anterior Body Vertical	22	0.84	<.0001	0.65	0.93
C5 Posterior Body Vertical	22	0.79	<.0001	0.55	0.91
C3 Anterior Body Vertical	18	0.77	0.0002	0.47	0.91
C4 Posterior Body Vertical	22	0.69	0.0003	0.38	0.86
C3 Posterior Body Vertical	19	0.56	0.0117	0.15	0.81
C5 Upper Angle AP	21	-0.46	0.0365	-0.74	-0.03
C3 Lower Angle AP	19	-0.51	0.0256	-0.78	-0.07
C5 Lower Angle AP	22	-0.53	0.0117	-0.78	-0.14
C4 Upper Angle AP	21	-0.59	0.0047	-0.82	-0.22
C4 Lower Angle AP	22	-0.68	0.0006	-0.85	-0.36

Subtracting the log of the inner lumen AP was performed in order to attempt to eliminate size differences between individuals. The values of these transformations are listed in Appendix D. The strongest correlations from this equation, in decreasing order, are: C4 anterior body vertical, C5 anterior body vertical, C5 posterior body vertical, C3 anterior body vertical, C3 anterior body vertical, C4 posterior body vertical, and C4 lower angle AP.

Forward stepwise regression analyses were completed with age as the outcome, and gender, C3, C4, and C5 log vertebral difference variables as the predictors. The final model included gender and log differences of C3 Upper AP Distance, C4 Anterior Body Vertical, C4 Upper Angle AP, and C5 Upper Angle Transverse. Attempting to fit models using quadratic and cubic terms for the difference variables did not result in a better fit.

Some factors changed together so that one could be substituted for the other. This resulted in the following equation as being predictive of bone age:

Equation:

Bone Age = 583.07-5.17*gender+50.14*logDif(C3 Upper AP Distance)+73.54*log Dif(C4 Anterior Body Vertical)-249.53*logDif(C4 Upper Angle AP)+120.49*logDif(C5 Upper Angle Transverse)

Where gender = 1 if female, 0 if male

For example, the bone age of subject 2 can be calculated as follows:

583.07-5.17+50.14*-0.225+73.54*-0.231-249.53*2.42+120.49*2.2 = 211 months.

As subject 2's true age is 204 months, her bone age is approximately 7 months accelerated.

Discussion

This study evaluated cross-sectional data from twenty-three individuals (fourteen female, nine male) in order to record linear and angular measurements changes occurring during growth on cervical vertebrae 3, 4, and 5. The goals of this study included reliable identification of points, as well as reliable measurements from these points on the vertebrae, and an objective assessment of morphologic changes, and the use of statistical models to predict age based on these measurements.

Measurement Error

The results of repeated point identification and measurements indicate a high concordance for point identification. Most of the measurements showed a Pearson Correlation of at least 0.9. Even though there were a few measurements that resulted in a lower correlation, these results were not statistically significant, and the actual differences between the first and second measurement were not clinically significant. This indicates that choosing points on the vertebrae according to clearly defined criteria is reliable and repeatable.

Correlations

Several of the correlations from this study are consistent with those previously described in the literature. For example, the Lower Angle AP measurement, indicative of vertebral "cupping," is indeed well correlated with age. However, the vertical heights (anterior and posterior) of the vertebral bodies show a stronger correlation with age than the lower AP angle. Of course, the lower angle is directly related to the vertical heights, as it is this increase in vertical size that results in the cupping of the vertebral body. Interestingly, the Upper Angle AP also shows a strong correlation with age, a measurement that has, to date, not yet been reported in the literature.

Prediction Models

The ultimate goal of this study was to study the morphology of the vertebrae and to determine if a predictive model can be created to determine the age of the patient. Because different vertebrae between individuals can very greatly in size, simply measuring the size of these vertebrae can be misleading. In order to remove this systematic error, the measurements were log transformed, and then a stable measurement (Inner Lumen AP) was subtracted from these values. This allowed studying the changing measurements with age but allowed removal of size between individuals as a variable.

Removing between-subjects size from the equation, the remaining variables were used to create an equation to predict an individual's age. This equation can accurately predict the skeletal age in months of any given patient.

Conclusion

This study showed that there are significant and predictable changes in the three dimensional morphology of the cervical vertebrae associated with age, and that these changes can be used to predict the skeletal age of a given patient. The null hypothesis that there is no correlation between the 3-D measurements of the cervical vertebrae and age is, therefore, rejected. Further work is needed on longitudinal data in order to refine the findings of this study.

References

1. Shi H, Scarfe WC, Farman AG. Three-dimensional reconstruction of individual cervical vertebrae from cone-beam computed-tomography images. Am J Orthod Dentofacial Orthop 2007;131:426-432.
2. Fishman LS. Can cephalometric x-rays of the cervical column be used instead of hand-wrist x-rays to determine patient's maturational age? Am J Orthod Dentofacial Orthop 2002;122:18A-19A.
3. Fishman LS. Chronological versus skeletal age, an evaluation of craniofacial growth. Angle Orthod 1979;49:181-189.
4. Hagg U, Taranger J. Maturation indicators and the pubertal growth spurt. Am J Orthod 1982;82:299-309.
5. Hagg UM, L. Dental maturity as an indicator of chronological age: the accuracy and precision of three models. Eur J Orthod 1985:25-34.
6. Sierra AM. Assessment of dental and skeletal maturity. A new approach. Angle Orthod 1987;57:194-208.
7. Green L. The interrelationships among height, weight and chronological, dental and skeletal ages. Angle Orthod 1961:189-193.
8. Tanner J, Whitehouse, RH, Marubini, E, Resele, LF. The adolescent growth spurt of boys and girls of the Harpenden growth study. Ann Hum Biol 1976:109-126.
9. Fishman LS. Radiographic evaluation of skeletal maturation. A clinically oriented method based on hand-wrist films. Angle Orthod 1982;52:88-112.
10. Grave KC, Brown T. Skeletal ossification and the adolescent growth spurt. Am J Orthod 1976;69:611-619.
11. Baccetti T, Franchi L, McNamara JA, Jr. An improved version of the cervical vertebral maturation (CVM) method for the assessment of mandibular growth. Angle Orthod 2002;72:316-323.
12. Franchi L, Baccetti T, McNamara JA, Jr. Mandibular growth as related to cervical vertebral maturation and body height. Am J Orthod Dentofacial Orthop 2000;118:335-340.
13. Garcia-Fernandez P, Torre H, Flores L, Rea J. The cervical vertebrae as maturational indicators. J Clin Orthod 1998;32:221-225.
14. Lamparski D. Skeletal Age Assessment Utilizing Cervical Vertebrae. Orthodontics. Pittsburgh PA: The University of Pittsburgh; 1972.
15. Zacharias L, Rand WM. Adolescent growth in height and its relation to menarche in contemporary American girls. Ann Hum Biol 1983;10:209-222.
16. Hassel B, Farman AG. Skeletal maturation evaluation using cervical vertebrae. Am J Orthod Dentofacial Orthop 1995;107:58-66.
17. Kucukkeles N, Acar A, Biren S, Arun T. Comparisons between cervical vertebrae and hand-wrist maturation for the assessment of skeletal maturity. J Clin Pediatr Dent 1999;24:47-52.
18. San Roman P, Palma JC, Oteo MD, Nevado E. Skeletal maturation determined by cervical vertebrae development. Eur J Orthod 2002;24:303-311.
19. Dhillon A. The Correlation of Cervical Vertebrae Maturation with Hand-Wrist Maturation and Statue Increments in Adolescent Girls. Alberta: University of Alberta; 1993.

20. O'Reilly MT, Yanniello GJ. Mandibular growth changes and maturation of cervical vertebrae--a longitudinal cephalometric study. Angle Orthod 1988;58:179-184.
21. Gray H, Standring S. Gray's Anatomy : The Anatomical Basis of Clinical Practice. Edinburgh: Elsevier Churchill Livingstone; 2005. Reprinted with permission from Elsevier.
22. DeLuca SA, Rhea JA. Radiographic anatomy of the cervical vertebrae. Med Radiogr Photogr 1980;56:18-24.
23. Bjork A, Helm S. Prediction of the age of maximum puberal growth in body height. Angle Orthod 1967;37:134-143.
24. Hellsing E. Cervical vertebral dimensions in 8-, 11-, and 15-year-old children. Acta Odontol Scand 1991;49:207-213.
25. Wang JC, Nuccion SL, Feighan JE, Cohen B, Dorey FJ, Scoles PV. Growth and development of the pediatric cervical spine documented radiographically. J Bone Joint Surg Am 2001;83-A:1212-1218.
26. Bench R. Growth of the cervical vertebrae as related to tongue, face and denture behaviour. Am J Orthod 1952:183-214.
27. Knutsson F. Growth and differentiation of the postnatal vertebra. Acta Radiol 1961;55:401-408.
28. Bick EM, Copel JW. Longitudinal growth of the human vertebra; a contribution to human osteogeny. J Bone Joint Surg Am 1950;32:803-814.
29. Abbassi V. Growth and normal puberty. Pediatrics 1998;102:507-511.
30. Franchi L, Baccetti T, McNamara JA, Jr. Thin-plate spline analysis of mandibular growth. Angle Orthod 2001;71:83-89.
31. Bambha JK. Longitudinal cephalometric roentgenographic study of face and cranium in relation to body height. J Am Dent Assoc 1961;63:776-799.
32. Bjork A. Sutural growth of the upper face studied by the implant method. Acta Odontol Scand 1966;24:109-127.
33. Brown T, Barrett MJ, Grave KC. Facial growth and skeletal maturation at adolescence. Tandlaegebladet 1971;75:1211-1222.
34. Lewis AB, Roche AF, Wagner B. Growth of the mandible during pubescence. Angle Orthod 1982;52:325-342.
35. Nanda R. The rates of facial growth of several facial components measured from serial cephalometric roentgenograms. Am J Orthod 1955:658-673.
36. Hunter CJ. The correlation of facial growth with body height and skeletal maturation at adolescence. Angle Orthod 1966;36:44-54.
37. Sato K. [Growth timing of mandibular length, body height, hand bones and cervical vertebrae during puberty]. Nippon Kyosei Shika Gakkai Zasshi 1987;46:517-533.
38. Hagg U, Pancherz H. Dentofacial orthopaedics in relation to chronological age, growth period and skeletal development. An analysis of 72 male patients with Class II division 1 malocclusion treated with the Herbst appliance. Eur J Orthod 1988;10:169-176.
39. Baumrind S, Frantz RC. The reliability of head film measurements. 1. Landmark identification. Am J Orthod 1971;60:111-127.

40. Baumrind S, Frantz RC. The reliability of head film measurements. 2. Conventional angular and linear measures. Am J Orthod 1971;60:505-517.
41. Bjork A, Solow B. Measurement on radiographs. J Dent Res 1962;41:672-683.
42. Carlsson CA. Imaging modalities in x-ray computerized tomography and in selected volume tomography. Phys Med Biol 1999;44:R23-56.
43. Hatcher DC, Aboudara CL. Diagnosis goes digital. Am J Orthod Dentofacial Orthop 2004;125:512-515.
44. Sukovic P. Cone beam computed tomography in craniofacial imaging. Orthod Craniofac Res 2003;6 Suppl 1:31-36; discussion 179-182.
45. Stratemann S. 3-D Craniofacial Imaging: Airway and Craniofacial Morphology. Oral and Craniofacial Sciences. San Francisco: University of California San Francisco; 2005: p. 368.
46. Meehan M, Teschner M, Girod S. Three-dimensional simulation and prediction of craniofacial surgery. Orthod Craniofac Res 2003;6 Suppl 1:102-107.
47. Yamamoto K, Ueno K, Seo K, Shinohara D. Development of dento-maxillofacial cone beam X-ray computed tomography system. Orthod Craniofac Res 2003;6 Suppl 1:160-162.
48. Araki K, Maki K, Seki K, Sakamaki K, Harata Y, Sakaino R et al. Characteristics of a newly developed dentomaxillofacial X-ray cone beam CT scanner (CB MercuRay): system configuration and physical properties. Dentomaxillofac Radiol 2004;33:51-59.
49. Kitaura H, Yonetsu K, Kitamori H, Kobayashi K, Nakamura T. Standardization of 3-D CT measurements for length and angles by matrix transformation in the 3-D coordinate system. Cleft Palate Craniofac J 2000;37:349-356.
50. Matteson SR, Bechtold W, Phillips C, Staab EV. A method for three-dimensional image reformation for quantitative cephalometric analysis. J Oral Maxillofac Surg 1989;47:1053-1061.
51. Graber TM, Vanarsdall RL, Vig KWL. Orthodontics : current principles & techniques. St. Louis, Mo.: Elsevier Mosby; 2005.

Appendix A: Raw Data Collected on each Subject

Subject	Gender	Months	C3 Anterior Body Vertical	C3 Posterior Body Vertical	C3 Upper AP Distance	C3 Lower AP Distance	C3 Upper Angle AP	C3 Upper Angle Transverse	C3 Lower Angle AP	C3 Lower Angle Transverse
1	F	220	13.664	13.015	10.75	12.72	171	124	150	160
2	F	204	7.6517	10.85	10.6	10.402	174	146	163	178
3	M	210	10.918	11.314	9.6062	10.18	171	132	161	179
4	F	192								
5	F	212	12.086	10.404	9.3727	11.118	175	142	150	179
6	F	189								
7	M	161	12.124	11.464	9.3366	10.341	178	160	166	191
8	F	117	7.5814	8.9377	7.3055	8.6093	174	151	168	174
9	M	141	6.5244	7.099	10.743	10.325	199	139	169	189
10	M	177	13.334	12.381	11.286	12.651	197	137	147	185
11	M	147	7.3077	9.4023	9.0039	9.418	177	134	150	174
12	M	132								
13	F	157	10.75	11.181	10.531	10.832	170	122	146	179
14	F	187	12.577	12.819	9.1754	11.516	175	131	150	186
15	M	119	6.0416	8.9558	11.588	11.397	199	141	196	207
16	F	186	12.634	11.971	9.9736	12.171	169	130	150	178
17	F	174	9.5925	9.1244	9.4046	10.277	170	126	152	188
18	F	144	9.6635	11.474	10.508	12.312	178	140	154	178
19	F	109	5.7153	9.2921	11.387	11.504	210	142	185	202
20	F	110	6.1974	8.1714	9.4857	10.046	185	145	176	185
21	M	204		14.298		13.479			150	191
22	F	155								
23	M	132	6.2033	7.9395	10.425	10.157	188	130	169	184

Subject	Gender	Months	C3 Inner Lumen AP	C3 Inner Lumen Transverse	C4 Anterior Body Vertical	C4 Posterior Body Vertical	C4 upper AP Distance	C4 Lower AP Distance	C4 Upper Angle AP	C4 Upper Angle Transvers
1	F	220	13.382	21.44	13.408	12.531	10.091	13.561		
2	F	204	13.27	23.409	11.603	11.351	10.439	12.654	165	150
3	M	210	14.798	24.453	11.742	12.07	9.3473	10.408	165	112
4	F	192								
5	F	212	15.439	21.501	12.502	11.166	9.0961	10.887	174	141
6	F	189			10.309	10.809	10.985	11.082	170	130
7	M	161	16.591	24.348	9.8288	11.109	10.218	9.7206	189	142
8	F	117	17.212	21.838	7.131	7.2133	9.2411	9.7103	188	138
9	M	141	14.335	22.9	6.054	7.0084	11.102	10.603	190	136
10	M	177	15.002	21.435	9.2741	9.1084	10.61	12.039	175	111
11	M	147	13.984	21.55	9.6439	8.6053	11.1	10.314	186	133
12	M	132			5.7451	7.0939	11.902	11.671	185	142
13	F	157	13.972	23.664	10.283	10.654	11.689	12.061	191	126
14	F	187	14.315	20.946	11.522	12.01	10.23	11.473	174	136
15	M	119	13.833	22.486	5.8779	8.3976	10.923	11.57	193	128
16	F	186	13.255	22.606	11.449	10.902	10.126	12.281	173	125
17	F	174	14.833	22.333	10.48	10.283	9.3988	10.179	174	125
18	F	144	12.461	23.816	9.3197	12.202	12.419	13.118	188	139
19	F	109	11.117	20.255	6.7409	8.4458	10.628	11.024	215	127
20	F	110	13.949	18.177	5.1522	6.969	8.8298	9.788	189	135
21	M	204	14.288	23.605	13.43	13.388	13.307	13.76	182	135
22	F	155			9.3469	10.527	12.671	10.549	198	151
23	M	132	14.178	22.476	6.6181	8.6595	9.7997	10.215	187	132

Subject	Gender	Months	C4 Lower Angle AP	C4 Lower Angle Transverse	C4 Inner Lumen AP	C4 Inner Lumen Transverse	C5 Anterior Body Vertical	C5 Posterior Body Vertical	C5 Upper AP Distance	C5 Lower / Distance
1	F	220	153	191	14.628	21.984	11.811	12.344	10.721	15.089
2	F	204	154	176	14.624	24.207	11.296	11.675	10.475	12.802
3	M	210	145	188	15.567	24.454	11.779	11.966	9.0503	10.717
4	F	192					10.511	11.351	11.245	11.326
5	F	212	154	174	14.409	12.679	11.32	12.05	9.4279	12.447
6	F	189	163	179	13.999	24.478	10.476	10.86	9.8765	11.133
7	M	161	165	190	15.74	25.26	11.151	10.544	8.3912	9.3985
8	F	117	182	179	16.402	23.609	7.0306	8.0343	9.6048	9.684
9	M	141	184	185	14.962	23.295	6.1983	8.111	10.112	9.4119
10	M	177	163	183	16.125	22.507	11.167	12.056	10.559	12.102
11	M	147	153	174	14.242	24.827	7.0495	8.815	10.399	10.954
12	M	132	183	184	14.303	25.493	7.1875	7.9058	11.285	12.024
13	F	157	158	172	14.568	24.227	10.208	11.102	10.91	12.7
14	F	187	158	185	14.145	22.024	11.889	11.702	11.133	11.55
15	M	119	192	199	13.64	24.068	5.914	8.3058	11.849	12.471
16	F	186	156	173	13.173	23.775	10.487	10.071	10.055	11.937
17	F	174	151	185	15.13	22.026	10.162	11.031	9.3398	10.504
18	F	144	157	183	13.699	21.168	11.763	12.542	12.161	12.632
19	F	109	193	205	12.041	20.887	6.6768	8.4282	11.69	12.104
20	F	110	183	186	14.136	19.62	5.2912	7.1444	8.5149	9.985
21	M	204	160	174	13.754	23.569	11.959	13.224	11.815	13.395
22	F	155	170	183	15.806	23.889				
23	M	132	169	185	13.795	21.997	6.6442	8.7376	10.208	10.094

Subject	Gender	Months	C5 Upper Angle AP	C5 Upper Angle Transverse	C5 Lower Angle AP	C5 Lower Angle Transverse	C5 Inner Lumen AP	C5 Inner Lumen Transverse
1	F	220	174	139	162	188	13.952	22.892
2	F	204	166	141	164	171	15.65	24.006
3	M	210	164	126	145	175	15.654	23.663
4	F	192			150	176	15.39	24.235
5	F	212	178	141	161	174	14.115	23.063
6	F	189	176	135	169	178	16.52	23.843
7	M	161	177	151	163	187	16.65	24.847
8	F	117	190	144	177	190	16.771	23.876
9	M	141	191	143	173	176	15.614	23.54
10	M	177	169	132	166	170	16.23	23.403
11	M	147	175	131	177	178	14.768	25.088
12	M	132	194	148	183	184	15.222	26.243
13	F	157	167	129	151	167	15.285	23.288
14	F	187	172	129	163	188	13.928	22.156
15	M	119	193	129	191	187	14.458	23.59
16	F	186	173	133	148	165	13.415	22.093
17	F	174	174	133	151	174	14.999	23.218
18	F	144	164	125	144	175	14.803	24.327
19	F	109	205	150	196	191	12.554	20.654
20	F	110	186	133	186	180	14.633	20.238
21	M	204	170	127	151	174	15.065	24.028
22	F	155						
23	M	132	191	137	165	183	14.988	22.846

Appendix B: Intra-Observer Data

Subject	PREDICTOR	Difference	6	C3_Lower_angle_transverse		16	C3_lower_AP_distance	-0.1820
2	C3_Anterior_body_vertical	-0.0953	14	C3_Lower_angle_transverse	2.0000	18	C3_lower_AP_distance	0.3100
6	C3_Anterior_body_vertical		16	C3_Lower_angle_transverse	-2.0000	2	C3_upper_AP_distance	0.3150
14	C3_Anterior_body_vertical	0.1040	18	C3_Lower_angle_transverse	-1.0000	6	C3_upper_AP_distance	
16	C3_Anterior_body_vertical	0.1630	2	C3_Posterior_body_vertical	-0.2990	14	C3_upper_AP_distance	0.0515
18	C3_Anterior_body_vertical	-0.0308	6	C3_Posterior_body_vertical		16	C3_upper_AP_distance	0.4994
2	C3_Inner_lumen_AP	0.3770	14	C3_Posterior_body_vertical	0.0390	18	C3_upper_AP_distance	1.2510
6	C3_Inner_lumen_AP		16	C3_Posterior_body_vertical	0.0790	2	C4_Anterior_body_vertical	-0.3760
14	C3_Inner_lumen_AP	-0.0100	18	C3_Posterior_body_vertical	-0.1560	6	C4_Anterior_body_vertical	-0.2480
16	C3_Inner_lumen_AP	-0.0960	2	C3_Upper_angle_AP	3.0000	14	C4_Anterior_body_vertical	0.2920
18	C3_Inner_lumen_AP	0.1610	6	C3_Upper_angle_AP		16	C4_Anterior_body_vertical	0.4130
2	C3_Inner_lumen_Transverse	-0.4700	14	C3_Upper_angle_AP	-5.0000	18	C4_Anterior_body_vertical	-0.3460
6	C3_Inner_lumen_Transverse		16	C3_Upper_angle_AP	-2.0000	2	C4_Inner_lumen_AP	1.0030
14	C3_Inner_lumen_Transverse	0.2110	18	C3_Upper_angle_AP	-5.0000	6	C4_Inner_lumen_AP	0.8080
16	C3_Inner_lumen_Transverse	-0.2760	2	C3_Upper_angle_Transverse	-2.0000	14	C4_Inner_lumen_AP	-0.2770
18	C3_Inner_lumen_Transverse	1.1010	6	C3_Upper_angle_Transverse		16	C4_Inner_lumen_AP	-0.0730
2	C3_Lower_Angle_AP	1.0000	14	C3_Upper_angle_Transverse	-2.0000	18	C4_Inner_lumen_AP	-0.0270
6	C3_Lower_Angle_AP		16	C3_Upper_angle_Transverse	-5.0000	2	C4_Inner_lumen_Transverse	-0.2490
14	C3_Lower_Angle_AP	0.0000	18	C3_Upper_angle_Transverse	-15.0000	6	C4_Inner_lumen_Transverse	-0.0320
16	C3_Lower_Angle_AP	-3.0000	2	C3_lower_AP_distance	1.3180	14	C4_Inner_lumen_Transverse	-0.0100
18	C3_Lower_Angle_AP	4.0000	6	C3_lower_AP_distance		16	C4_Inner_lumen_Transverse	-0.4210
2	C3_Lower_angle_transverse	1.0000	14	C3_lower_AP_distance	0.0820	18	C4_Inner_lumen_Transverse	3.1170

2	C4_Lower_Angle_AP	-1.0000	18	C4_Upper_angle_Transverse	-5.0000	16	C5_Inner_lumen_Transverse	0.1150
6	C4_Lower_Angle_AP	0.0000	2	C4_lower_AP_distance	-0.4450	18	C5_Inner_lumen_Transverse	-0.3710
14	C4_Lower_Angle_AP	1.0000	6	C4_lower_AP_distance	-0.0870	2	C5_Lower_Angle_AP	1.0000
16	C4_Lower_Angle_AP	-1.0000	14	C4_lower_AP_distance	0.0410	6	C5_Lower_Angle_AP	-1.0000
18	C4_Lower_Angle_AP	0.0000	16	C4_lower_AP_distance	-0.1160	14	C5_Lower_Angle_AP	0.0000
2	C4_Lower_angle_transverse	3.0000	18	C4_lower_AP_distance	-0.2180	16	C5_Lower_Angle_AP	3.0000
6	C4_Lower_angle_transverse	-4.0000	2	C4_upper_AP_distance	0.1640	18	C5_Lower_Angle_AP	1.0000
14	C4_Lower_angle_transverse	4.0000	6	C4_upper_AP_distance	0.2560	2	C5_Lower_angle_transverse	2.0000
16	C4_Lower_angle_transverse	3.0000	14	C4_upper_AP_distance	0.2090	6	C5_Lower_angle_transverse	-3.0000
18	C4_Lower_angle_transverse	-1.0000	16	C4_upper_AP_distance	-0.0240	14	C5_Lower_angle_transverse	-6.0000
2	C4_Posterior_body_vertical	0.1330	18	C4_upper_AP_distance	0.8320	16	C5_Lower_angle_transverse	5.0000
6	C4_Posterior_body_vertical	0.5170	2	C5_Anterior_body_vertical	-0.1520	18	C5_Lower_angle_transverse	-5.0000
14	C4_Posterior_body_vertical	0.0200	6	C5_Anterior_body_vertical	-0.1360	2	C5_Posterior_body_vertical	-0.2420
16	C4_Posterior_body_vertical	0.4950	14	C5_Anterior_body_vertical	-0.0630	6	C5_Posterior_body_vertical	-0.1530
18	C4_Posterior_body_vertical	-0.0640	16	C5_Anterior_body_vertical	0.1690	14	C5_Posterior_body_vertical	0.2090
2	C4_Upper_angle_AP	1.0000	18	C5_Anterior_body_vertical	0.4870	16	C5_Posterior_body_vertical	0.5380
6	C4_Upper_angle_AP	-2.0000	2	C5_Inner_lumen_AP	-0.6870	18	C5_Posterior_body_vertical	0.0210
14	C4_Upper_angle_AP	2.0000	6	C5_Inner_lumen_AP	-0.9120	2	C5_Upper_angle_AP	-1.0000
16	C4_Upper_angle_AP	-3.0000	14	C5_Inner_lumen_AP	-0.0420	6	C5_Upper_angle_AP	-3.0000
18	C4_Upper_angle_AP	0.0000	16	C5_Inner_lumen_AP	1.1650	14	C5_Upper_angle_AP	-1.0000
2	C4_Upper_angle_Transverse	-5.0000	18	C5_Inner_lumen_AP	0.4430	16	C5_Upper_angle_AP	-4.0000
6	C4_Upper_angle_Transverse	-4.0000	2	C5_Inner_lumen_Transverse	1.3140	18	C5_Upper_angle_AP	2.0000
14	C4_Upper_angle_Transverse	0.0000	6	C5_Inner_lumen_Transverse	0.4120	2	C5_Upper_angle_Transverse	-3.0000
16	C4_Upper_angle_Transverse	-6.0000	14	C5_Inner_lumen_Transverse	0.1910	6	C5_Upper_angle_Transverse	-9.0000

14	C5_Upper_angle_Transverse	-1.0000	14	C5_lower_AP_distance	0.0660	14	C5_upper_AP_distance	-0.1220
16	C5_Upper_angle_Transverse	-11.0000	16	C5_lower_AP_distance	-0.0320	16	C5_upper_AP_distance	-0.2053
18	C5_Upper_angle_Transverse	-4.0000	18	C5_lower_AP_distance	0.0250	18	C5_upper_AP_distance	0.2300
2	C5_lower_AP_distance	-0.0590	2	C5_upper_AP_distance	0.7880			
6	C5_lower_AP_distance	0.5610	6	C5_upper_AP_distance	0.3555			

Appendix C: Summary Data for Patients

Variable	Mean	SD	Median	Min	Max
Age (months)	164.30	35.05	161.00	109.00	220.00
Age (years)	13.35	2.87	13.00	9.00	18.00
C3 Anterior Body Vertical	9.48	2.84	9.63	5.72	13.66
C3 Inner Lumen AP	14.22	1.35	14.18	11.12	17.21
C3 Inner Lumen Transverse	22.28	1.53	22.48	18.18	24.45
C3 Lower Angle AP	160.63	13.96	154.00	146.00	196.00
C3 Lower Angle Transverse	183.53	10.42	184.00	160.00	207.00
C3 Posterior Body Vertical	10.53	1.94	10.85	7.10	14.30
C3 Upper Angle AP	181.11	12.37	176.00	169.00	210.00
C3 Upper Angle Transverse	137.33	9.79	138.00	122.00	160.00
C3 Lower AP Distance	11.02	1.25	10.83	8.61	13.48
C3 Upper AP Distance	10.03	1.05	10.20	7.31	11.59
C4 Anterior Body Vertical	9.43	2.57	9.74	5.15	13.43
C4 Inner Lumen AP	14.49	1.03	14.36	12.04	16.40
C4 Inner Lumen Transverse	22.73	2.70	23.59	12.68	25.49
C4 Lower Angle AP	165.73	14.21	161.50	145.00	193.00
C4 Lower Angle Transverse	183.32	8.30	183.50	172.00	205.00
C4 Posterior Body Vertical	10.02	1.97	10.59	6.97	13.39
C4 Upper Angle AP	183.38	11.91	186.00	165.00	215.00
C4 Upper Angle Transverse	133.05	10.24	135.00	111.00	151.00
C4 Lower AP Distance	11.30	1.22	11.05	9.71	13.76
C4 Upper AP Distance	10.64	1.20	10.52	8.83	13.31
C5 Anterior Body Vertical	9.45	2.37	10.48	5.29	11.96
C5 Inner Lumen AP	15.03	1.05	15.03	12.55	16.77
C5 Inner Lumen Transverse	23.42	1.33	23.57	20.24	26.24
C5 Lower Angle AP	165.27	15.03	163.50	144.00	196.00
C5 Lower Angle Transverse	178.68	7.58	177.00	165.00	191.00
C5 Posterior Body Vertical	10.36	1.84	10.95	7.14	13.22
C5 Upper Angle AP	178.52	11.53	175.00	164.00	205.00
C5 Upper Angle Transverse	136.00	7.92	133.00	125.00	151.00
C5 Lower AP Distance	11.57	1.42	11.74	9.40	15.09
C5 Upper AP Distance	10.40	1.07	10.44	8.39	12.16

Appendix D: Log transformed data subtracted from Log Inner Lumen AP

Subject	Gender	age_months	DIF_C3_upper_AP_distance	DIF_C4_Anterior_body_vertical	DIF_C4_Upper_angle_AP	DIF_C5_Upper_angle_Transverse
1	F	220	-0.219004766	-0.087085957		2.298851066
2	F	204	-0.224651847	-0.231400329	2.423281459	2.198288973
3	M	210	-0.432083313	-0.281981131	2.360792185	2.085555432
4	F	192				
5	F	212	-0.499095567	-0.14196438	2.491202288	2.301521829
6	F	189		-0.305968598	2.496812539	2.10070301
7	M	161	-0.574918219	-0.470888392	2.485541772	2.20486962
8	F	117	-0.856979326	-0.832951802	2.439038684	2.150162095
9	M	141	-0.28844972	-0.904794443	2.541510419	2.214676683
10	M	177	-0.284620506	-0.553145294	2.384415111	2.095940541
11	M	147	-0.440256002	-0.389869754	2.569551328	2.182734645
12	M	132		-0.912121988	2.55988652	2.274470524
13	F	157	-0.282732039	-0.348335296	2.573446086	2.132940449
14	F	187	-0.444781949	-0.205102953	2.509694094	2.225911202
15	M	119	-0.177086962	-0.841807097	2.649683536	2.18856451
16	F	186	-0.284433238	-0.14026689	2.575122314	2.293975644
17	F	174	-0.455655497	-0.367210849	2.442375771	2.182365596
18	F	144	-0.170466895	-0.385192398	2.619119125	2.133483874
19	F	109	0.023996886	-0.580124046	2.882320535	2.480595954
20	F	110	-0.38562242	-1.009300927	2.59302228	2.207069876
21	M	204		-0.02383868	2.582676996	2.131812914
22	F	155		-0.525344877	2.527877416	
23	M	132	-0.3074847	-0.734497888	2.606802409	2.212731045